Published in final edited form as:
Neuroimage. 2007 February 1; 34(3): 905–923.

Sequence of information processing for emotions based on the anatomic dialogue between prefrontal cortex and amygdala

H. T. Ghashghaei[a,e], **C. C. Hilgetag**[a,d], and **H. Barbas**[a,b,c,*]

a *Boston University, Boston, MA*

b *Program in Neuroscience, Boston University and School of Medicine, Boston, MA*

c *New England Primate Research Centre, Harvard Medical School, Southborough, MA, USA*

d *School of Engineering and Science, International University Bremen, Campus Ring 6, RII-116, D-28759, Bremen, Germany.*

The prefrontal cortex and the amygdala have synergistic roles in regulating purposive behavior, effected through bidirectional pathways. Here we investigated the largely unknown extent and laminar relationship of prefrontal input-output zones linked with the amygdala using neural tracers injected in the amygdala in rhesus monkeys. Prefrontal areas varied vastly in their connections with the amygdala, with the densest connections found in posterior orbitofrontal and posterior medial cortices, and the sparsest in anterior lateral prefrontal areas, especially area 10. Prefrontal projection neurons directed to the amygdala originated in layer 5, but significant numbers were also found in layers 2 and 3 in posterior medial and orbitofrontal cortices. Amygdalar axonal terminations in prefrontal cortex were most frequently distributed in bilaminar bands in the superficial and deep layers, by columns spanning the entire cortical depth, and less frequently as small patches centered in the superficial or deep layers. Heavy terminations in layers 1−2 overlapped with calbindin positive inhibitory neurons. A comparison of the relationship of input to output projections revealed that among the most heavily connected cortices, cingulate areas 25 and 24 issued comparatively more projections to the amygdala than they received, whereas caudal orbitofrontal areas were more receivers than senders. Further, there was a significant relationship between the proportion of 'feedforward' cortical projections from layers 2−3 to 'feedback' terminations innervating the superficial layers of prefrontal cortices. These findings indicate that the connections between prefrontal cortices and the amygdala follow similar patterns as corticocortical connections, and by analogy suggest pathways underlying the sequence of information processing for emotions.

The amygdala and the prefrontal cortex have synergistic roles in regulating purposive behavior [(Schoenbaum et al., 2000;Izquierdo and Murray, 2005); reviewed in (Barbas, 2000;Bechara et al., 2000)]. The amygdala appears to extract the affective significance of stimuli, and the prefrontal cortex guides goal-directed behavior (Damasio, 1994;Petrides, 1996;Roberts and Wallis, 2000;Levy and Goldman-Rakic, 2000;Fuster, 2000;Barbas et al., 2002). Communication between the amygdala and the prefrontal cortex is bidirectional [e.g., (Nauta, 1961;Pandya et al., 1973;Jacobson and Trojanowski, 1975;Aggleton et al., 1980;Porrino et al.,

[e]Current address: Department of Molecular Biomedical Sciences, School of Veterinary Medicine, North Carolina State University, Raleigh, NC.
[*]Corresponding author. Dept. Health Sciences, Boston University, 635 Commonwealth Ave. Room 431, Boston, MA 02215. E-mail address: barbas@bu.edu

1981;Van Hoesen, 1981;Amaral and Price, 1984;Barbas and De Olmos, 1990;Morecraft et al., 1992;Carmichael and Price, 1995), and appears to be essential in judging rewarding or aversive outcomes of actions [e.g., (Bechara et al., 1997;Schoenbaum et al., 1998)]. Posterior orbitofrontal cortex, in particular, has highly specific connections in the amygdala, including distinct input and output zones, which differ markedly from the connections of either anterior cingulate or lateral prefrontal cortices (Ghashghaei and Barbas, 2002).

There is, however, considerable uncertainty on the organization of the complementary part of this interaction, namely input and output zones in prefrontal cortices connected with the amygdala. Qualitative studies have shown that projections from the amygdala terminate in layers 2 and 5 in prefrontal areas of monkeys (Porrino et al., 1981;Amaral and Price, 1984) and rats (Bacon et al., 1996), and cortical projections to the amygdala arise primarily from the deep layers (Aggleton et al., 1980;Ottersen, 1982;Russchen, 1982;Cassell et al., 1989;Stefanacci et al., 1996). However, the prefrontal cortex in primates is complex, composed of lateral prefrontal areas, associated with cognitive processes, and orbitofrontal and anterior cingulate cortices, which have a role in emotional processes [reviewed in (Barbas et al., 2002)]. There is no information on whether laminar-specific connections link these functionally distinct prefrontal cortices with the amygdala.

The laminar distribution of connections has important implications for neural processing, because pathways terminating in different layers vary substantially in synaptic features and encounter distinct types of inhibitory interneurons [e.g., (Barbas et al., 2005b;Germuska et al., 2006)]. Moreover, laminar-specific connections can be used to infer the flow of information by analogy with sensory cortices. Feedforward projections originate from neurons in layers 2−3 of earlier-processing sensory areas, and innervate the middle layers of later-processing sensory areas [reviewed in (Felleman and Van Essen, 1991)]. Feedback projections proceed in the opposite direction, and originate mostly from neurons in layers 5−6 and terminate most densely in layer 1.

Corticocortical connections, however, are notoriously complex: They can originate from layers 2−3, and 5−6 and terminate in layers 1−6 in varied proportions. We previously demonstrated that the relative laminar distribution of connections linking pairs of prefrontal cortices is highly correlated with the relationship of the areas' structure (Barbas and Rempel-Clower, 1997). The structure of different cortical areas is assessed quantitatively by the number of identifiable layers or overall neuronal density (Dombrowski et al., 2001;Medalla and Barbas, 2006). According to the structural model, 'feedforward' connections originate from a type of cortex with more layers or higher cell density than the cortex of destination and 'feedback' connections reflect the opposite relationship. Further, the structural model is relational, so that the relative laminar distribution of connections in pairs of linked areas is correlated with the relative difference in their structure. Here we exploited the power of the structural model to summarize succinctly complex patterns of cortical connections in order to investigate whether the input and output zones that link the laminated prefrontal cortex with the non-laminated nuclei of the amygdala follow similar rules as corticocortical connections.

Materials and methods

Experiments were conducted on 4 adult rhesus monkeys (*Macaca mulatta*) of both sexes, obtained through the New England Regional Primate Research Center (NEPRC). Experiments were conducted according to the NIH guide for the Care and Use of Laboratory Animals (NIH publication 86−23, revised 1987). Experimental methods and euthanasia were approved by the IACUC at NEPRC, Harvard Medical School, and Boston University School of Medicine. All efforts were made to minimize animal suffering and to reduce their number.

Stereotaxic coordinates of the amygdala

Prior to surgery for injection of tracers, we calculated the coordinates for the amygdala using magnetic resonance imaging (MRI). The interaural line was used as reference and was marked by filling hollow ear bars of the stereotax with betadine salve that is visible in MRI. Brain scans were obtained from monkeys sedated with ketamine hydrochloride (10 mg/kg, intramuscularly) and then anesthetized with sodium pentobarbital, administered intravenously through a femoral catheter (to effect). A T1 weighted 3D SPGR (TR70 ms, TE6 ms, Flip 45°) was obtained through the amygdala using 512 × 384 matrices and 16 × 16 FOVs. The stereotaxic coordinates for the amygdala were calculated in three dimensions using the interaural line as reference. The medio-lateral coordinates were calculated relative to the midline of the brain running through the longitudinal fissure.

Surgical procedures

Surgery for injection of neural tracers was conducted immediately after, or one week after MRI. The monkeys were anesthetized with ketamine hydrochloride (10−15 mg/kg, intramuscularly), intubated and anesthetized with isofluorane until a surgical level of anesthesia was accomplished. The monkeys were then placed in the same stereotaxic apparatus used for imaging and a small region of the cortex above the desired target was exposed. Surgery was performed under aseptic conditions while heart rate, muscle tone, respiration, and pupillary dilatation were closely monitored. A small opening was made in the skull and the dura for the penetration of the needle to the amygdala.

Injection of neural tracers—The goal was to investigate the areal and laminar organization of connections linking prefrontal cortices with the amygdala. This was accomplished by placing tracers in the amygdala to map efferent and afferent connections in distinct prefrontal cortices. To study the zones in the prefrontal cortices connected with the amygdala, we injected the bidirectional tracer biotinylated dextran amine (BDA, Molecular Probes, Eugene, OR, CAT# D-7135) in four hemispheres of two animals (cases BBr, BBl, BDr, BDl), as described in Table 1. We previously found that connections between prefrontal cortices and the amygdala are strictly ipsilateral in rhesus monkeys (Ghashghaei and Barbas, 2002), as they are in rats (Cassell et al., 1989), so injections in two hemispheres in the same animal can be considered independent. We injected tracers using a microsyringe (10 mg/ml, 10 μl total; Hamilton, Reno, NV, CAT#80383) mounted on a microdrive. BDA is an excellent anterograde tracer that labels the entire extent of axonal terminals and boutons. BDA also labels neurons retrogradely, particularly in the 3000 MW form (Veenman et al., 1992;Reiner et al., 2000).

To confirm the retrograde results from the BDA injections, we placed injections of other reliable bidirectional (fluororuby, dextran tetramethylrhodamine, 1−2 μl of 2 mg/ml, MW 3000, Molecular Probes; CAT#D-3308), or retrograde (fast blue, 1 μl of 2 mg/ml, Sigma, St. Louis, MO, CAT#F5756) fluorescent tracers in the amygdala in one hemisphere in each of three monkeys (cases BBb; AW; AX), as described in Table 1. In all cases in this study, 1−3 penetrations were made from the top of the brain to the calculated depths in the amygdala. A period of 10−15 minutes was allowed for each injection, in order to allow the dye to penetrate at the injection site and avoid uptake of the dye upon retraction of the needle. The contralateral hemisphere in cases AW and AX was used to investigate connections in studies unrelated to the present study, using different tracers.

Perfusion and tissue processing

The survival period was 14−18 days. The animals were then anesthetized and perfused through the heart with 4% paraformaldehyde, and the brains were removed from the skull, photographed, cryoprotected in sucrose (10−30%), and cut at 50 μm on a freezing microtome, as described previously (Barbas et al., 2005b).

In experiments with BDA injections, one series of sections was processed to visualize boutons and labeled neurons as described previously (Barbas et al., 2005b;Zikopoulos and Barbas, 2006). BDA labeled neurons and terminals were also labeled for immunofluorescence using avidin conjugated probes for visualizing the transported dextran (AlexaFluoro-AvidinD; Molecular Probes). In order to simultaneously visualize neurons and axonal terminals labeled with BDA and neurons and fibers positive for calcium binding proteins, we used standard immunocytochemical techniques to visualize calbindin (CB) or parvalbumin (PV) positive neurons as described previously (Barbas et al., 2005b).

Data analysis

Mapping projection neurons—Sections through the prefrontal cortex ipsilateral to the injection sites were viewed under a microscope (Olympus, BX 60) using brightfield or fluorescence illumination and labeled neurons were mapped quantitatively using a semi-automated commercial system with a motorized stage and software (Neurolucida, Microbrightfield, Colchester, VT). The terminology for the architectonic areas of the prefrontal cortices was based on the map of Barbas and Pandya (Barbas and Pandya, 1989), and the quantitative architecture of prefrontal cortices (Dombrowski et al., 2001). Borders of prefrontal architectonic areas and their layers were delineated in the same sections counterstained with thionin.

Mapping anterograde label—We mapped the distribution of labeled boutons in the prefrontal cortices under a microscope (Olympus BX60) using brightfield illumination and the Neurolucida software in cases with injections of BDA. We then employed standard stereological procedures to estimate the areal and laminar density of boutons, using the optical fractionator according to the method described by West and Gundersen [e.g., (Gundersen et al., 1988;West and Gundersen, 1990)]. Briefly, the method is based on an unbiased estimate of the density of objects (boutons here), where every bouton has an equal opportunity of being counted, and no bouton can be counted twice. Data for stereological analyses were obtained using a semi-automated commercial system and software (StereoInvestigator, Microbrightfield, Colchester, VT). We first conducted a pilot study on a subset of areas and layers (14 areas) to obtain optimal parameters to estimate the number of boutons in each layer of every area of the prefrontal cortex. The pilot study indicated that at 600X magnification, using 200−400 μm sampling grids (depending on the thickness of the layers), 45 × 45 μm counting frames, and 10−12 sampling sites for every layer in 3 sections, consistently resulted in reliable bouton estimates with a coefficient of error (CE) below 10%.

The data are based on a sampling size that exceeded by 50% the requirements of the pilot study (four animals, four sections, 10−12 sampling sites for each layer of each area). The sizes of the sampling grids varied among different layers, but were kept constant for each layer of specific areas across cases. The counting frames included exclusion and inclusion zones to avoid overestimating, as well as guard zones (2 μm each on top and bottom of the sections) to avoid error due to plucked boutons at the cut edge of sections (Williams and Rakic, 1988).

In each animal, coronal sections through rostral to caudal extent of the prefrontal cortex were numbered and architectonic areas within each section identified. For each area, four sections were selected using systematic random sampling to count boutons in each layer. The data included planemetric volume calculations for each layer, which take into consideration the area of the layer and thickness of each section. The volume estimates along with the total estimates of bouton numbers were used to calculate the density of boutons per unit volume (mm^3) in each animal.

Normalization of data—We normalized data for two sets of analyses: to compute the percentage of boutons across layers for each area; and to compute the relative density of boutons across all areas with label for a given injection site. Within area normalization does not reveal density differences across areas except by laminar pattern, whereas across area normalization does. We used the normalized bouton data for comparison with percentage of projection neurons in order to compare the contribution of each area to input and output connections of the prefrontal cortex with the amygdala. We used standard statistical tests (single-factor ANOVA; factor: structural type, 4 levels) to test for significant differences in the connections of different prefrontal areas with the amygdala.

We used a hierarchical cluster analysis to assess the relative similarity of different injections in the amygdala, based on the resulting patterns of retrograde labeling in prefrontal cortices. The pair wise similarity of the patterns was evaluated by Pearson's correlation of the relative labeling density in all prefrontal areas. Clusters were joined based on the centroid linkage method in the hierarchical cluster routine of the SYSTAT statistical package (v.11, Systat Software, Inc., Point Richmond, CA, USA). The resulting cluster organization was represented as a hierarchical tree diagram, in which large clustering distances (at the root of the tree) indicate smaller similarity of the data, and smaller distances (towards the endpoints of the branches) indicate greater similarity of the data. Therefore, as one proceeds from the root of the tree to its endpoints, one large all-inclusive cluster segregates into several smaller components, containing more similar data. At the finest resolution (i.e., shortest clustering distance, corresponding to greatest similarity), all data are assigned to their individual clusters.

Density analysis summary on reconstructed prefrontal hemispheres—Retrograde and anterograde data for each prefrontal area from all cases were pooled in matched coronal sections. A total of 10 sections spaced equally (approximately 4−5 sections apart in the stained series) were selected and the density data were averaged across matched sections in all cases. These calculations generated 10 averaged densities spanning the rostral to caudal extent of the prefrontal cortex, representing 10 equidistant rostro-caudal levels of the prefrontal cortex. The range of averaged densities was then normalized on a scale of 1 to 100 (1, lowest density; 100, highest density) and the densities were assigned pseudo-color codes as follows: 1−25, blue; 26−50, green; 51−75, yellow; and 76−100, red, in each area and in each of the 1 −10 levels. The density values were then reconstructed on photographs of the medial, orbitofrontal, and lateral prefrontal surfaces, showing the relative density in pseudo-color using Adobe Illustrator. The representative equidistant averages were used to fill the gaps between each of the sequential levels in the maps generated. Densities were summarized for gyral but not sulcal areas.

Analysis of the relationship of CB/PV interneurons in the prefrontal cortices with projection neurons directed to the amygdala—We studied the relationship of projection neurons to local inhibitory interneurons, marked by the calcium binding proteins CB and PV. This was accomplished by counting the number of neurons positive for CB or PV within a 75 μm radius around each labeled projection neuron in the prefrontal cortices using the Neurolucida software. The 75 μm radius was chosen after a pilot study showed that it reflected the average distance between labeled projection neurons.

Delineation of prefrontal areas and their layers—We delineated architectonic borders of prefrontal areas from coronal sections counterstained for Nissl, according to the map of Barbas and Pandya (Barbas and Pandya, 1989). We separated the ventral and dorsal parts of area 24 (V24, D24), which constituted the only additions to the areas of the above map.

In areas 24, 32, 25 and 13, we considered the acellular gap between the deep and superficial layers as the middle layer. However, the medial periallocortex (area MPAll), orbital

periallocortex (area OPAll) and orbital proisocortex (area OPro) have neither a distinct layer 4, nor the acellular gap between the superficial and deep layers, hence layer 4 is not depicted for them. Thus, the middle layers of MPAll, OPAll and OPro included the deep part of layer 3 and superficial part of layer 5. We mapped injection sites in the amygdala on coronal sections, and delineated the nuclei according to maps of the amygdala (Price et al., 1987;De Olmos, 1990).

Photography—Photomicrographs for presentation of data were captured directly from histological brain slides using a CCD camera and the Neurolucida Virtual Slice software, and were imported into Adobe Photoshop for assembly, labeling, and adjustment of overall brightness, but were not retouched. Double labeled tissue was visualized using confocal microscopy (Olympus).

Results

Injection sites

In one group of experiments (n=3) retrograde fluorescent tracers occupied restricted sites of the basal nuclei of the amygdala (Figs. 1B-D, Table 1). In a second group of experiments (n=4 hemispheres) the bidirectional tracer BDA occupied extensive parts of the basal complex of the amygdala (Figs. 1A-B; D-F; A'-E'). In all cases, labeled projection neurons and axonal terminals were found in nearly all prefrontal areas, but varied in density in areas and distinct layers, as elaborated below.

Prefrontal projection neurons directed to the amygdala

Caudal medial and orbitofrontal areas issued the most robust projections to the amygdala (Figs. 2-4), as summarized for pooled data and mapped in Figure 5. The highest densities of projection neurons were noted in medial area 25 (M25), dorsal area 24 (D24), and the orbitofrontal area OPro, in spite of the fact that the injection sites were centered in different parts of the amygdala (Figs. 2C-D, G-H, K-L; 3F-H; 4E-H; 5A,C, D, F). A cluster analysis based on the profile of projections resulting from different injection sites showed that cases with a predominant involvement of the medial nuclei clustered together, while those involving principally the basolateral (BL) nucleus formed another cluster (Fig. 5E). This confirmed the consistency of labeling after injection of specific sectors of the amygdala.

The specificity of projections to restricted sites of the amygdala was evident after an injection confined to the basomedial nucleus (BM, also known as accessory basal; Fig. 2A-D), which resulted in large numbers of projection neurons in the medial part of area 25 (M25, 53%). Area 24 included a substantial proportion of labeled neurons (33−36%) when the tracer injection included the ventrolateral part of BL and a small part of the adjacent part of the lateral (L) nucleus (Fig. 1B, case BB_L; Fig. 1C, case AW_L).

As in medial prefrontal areas, most projection neurons from orbitofrontal cortex were found in its posterior sector. Area OPro included the highest proportion of projection neurons directed to the amygdala (Figs. 2D; 3-5), especially when injections included the intermediate part of the basolateral (BLi) nucleus (20−23%). The adjacent orbital area OPAll, area 13, and orbital area 12 (O12) also included moderate numbers of projection neurons directed to the amygdala. Rostral orbitofrontal cortices, including orbital area 14 (O14), 11, and orbital area 25 (O25) issued lighter projections (Figs. 2-4).

Overall, projections from lateral prefrontal cortices were significantly sparser than from medial and orbitofrontal areas, and most arose from the ventrolaterally situated area 12 (L12; Figs. 2-4). Ventral area 46 (V46) also included a few labeled neurons in most cases, except one case

where the injection was restricted to the BM nucleus (Fig. 2A-D; case AX). Other lateral prefrontal areas included few, if any, labeled neurons, suggesting that lateral prefrontal projections to the amygdala originate primarily from its ventral sectors, and project preferentially to the basolateral nucleus of the amygdala. Area 10 stood apart from other areas with the sparsest projections to the amygdala emanating from either its medial or lateral sectors.

Caudal orbitofrontal and caudal medial prefrontal cortices differ in their laminar organization from rostral orbitofrontal, rostral medial, and lateral prefrontal areas, so we grouped data from different areas based on their cortical type into four categories, as follows: agranular cortices included those lacking layer 4 (areas MPAll and OPAll); dysgranular areas included areas with a poorly developed layer 4 (areas 24, 25, 32, 13, and OPro); eulaminate areas included those with six layers, which were divided into two groups: eulaminate I (areas 14, 11, 10, 12, and 9) and eulaminate II cortices (areas 8 and 46), based on the distinction of their 6 layers, which is higher in eulaminate II than in I (Dombrowski et al., 2001). This analysis revealed significant differences in projection density among different types of prefrontal cortices (single-factor ANOVA, $F(3,24) = 25.39$, $P<0.00001$).

Laminar organization of prefrontal projections to the amygdala—Normalized data from each case were pooled and are shown in Figure 5F. Most labeled neurons were found in cortical layer 5. Projection neurons in layers 2 and 3 were found in significant numbers only in caudal medial (areas MPAll, 32, 25, 24) and caudal orbitofrontal areas (OPAll, and OPro). Posterior orbitofrontal areas (areas OPAll, OPro) were distinguished by a comparable distribution of projection neurons in the upper (2−3) and deep (5−6) layers, as were caudal medial areas (MPAll, V24; Fig. 5F). Nevertheless, projections from superficial layers did not exceed projections from the deep layers in any prefrontal area. There were only a few labeled neurons in layer 6, found mostly in caudal medial and orbitofrontal areas, or in areas V46 and L12.

Axonal terminations from the amygdala in prefrontal cortices

We next investigated the extent of labeled axonal terminations from the amygdala in prefrontal cortices in four hemispheres of two animals with injection of BDA (cases BB and BD; Figs. 3-4). Prefrontal connections with the amygdala are ipsilateral, so terminations in each hemisphere are considered to be independent.

Axonal terminals from the amygdala were found in all areas and layers of the prefrontal cortex, but varied substantially in density across areas. The highest densities were found in caudal orbitofrontal and caudal medial prefrontal cortices (areas OPAll, OPro, M25, MPAll, and 24). In contrast, rostral orbitofrontal, rostral medial, and lateral prefrontal areas included considerably lower densities of boutons (Figs. 3, 4, 6A-D). Analysis of projection density of areas grouped into four categories according to cortical type (as described above) revealed that the density of axonal boutons from the amygdala differed significantly among different types of prefrontal cortices (single-factor ANOVA, $F(3,19) = 7.81$, $P < 0.01$). Caudal agranular and dysgranular cortices (found in the caudal orbitofrontal and medial prefrontal cortex) received the highest density of axonal terminals. In contrast, the density of terminations in eulaminate areas in rostral orbitofrontal, rostral medial and lateral prefrontal cortices was comparatively low.

Laminar pattern of terminations from the amygdala in prefrontal cortices—Axonal boutons from the amygdala assumed several distinguishable patterns. The most prominent pattern consisted of terminations distributed in two bands parallel to the pial surface. One band innervated superficial layers 1, 2, or both, and the other the deep part of layer 5 and layer 6 (Fig. 7A,D,G; red arrowheads). In another pattern, columns of axonal terminals

innervated all cortical layers. In caudal medial and orbitofrontal areas, the columns were broad (>1mm in w idth; Fig. 7H, green arrowheads), and small in anterior prefrontal areas (<1mm in width; Fig. 7D, green arrowheads). Another pattern showed patches of axonal terminals clustered in the superficial (layers 1, 2; Fig. 7C, yellow arrowheads), middle (layer 4 and surrounding parts of layers 3 and 5; Fig. 7G, yellow arrowhead), or deep (layers 5 and 6; Fig. 7F, yellow arrowheads) layers of the cortex. The patchy pattern of innervation was mostly seen in rostral prefrontal areas. In a few rostral areas (e.g., area O14), there was occasional unilaminar innervation of layer 1 (Fig. 7E; blue arrowhead).

We further investigated the laminar specificity of amygdalar innervation of prefrontal cortex using density data for individual layers of each area. Figure 6D shows the relative density of boutons across areas as well as their distribution within layers of each area. Layers 1 and 2 of most medial and orbitofrontal areas included the highest density of boutons. Caudal medial and orbitofrontal areas (areas MPAll, M25 and OPAll) had the highest density of labeled boutons in layer 1, while layer 2 of areas 24, OPro, L12, 32, 14, and medial area 9 (M9) was the most densely innervated (Fig. 6D). Other prefrontal cortices included relatively balanced densities of boutons in their superficial and deep layers, suggesting a true bilaminar innervation by the amygdala in these areas. In general, layer 6 of most lateral prefrontal areas included the highest density of boutons, except area D9, where layer 5 had the highest density. In addition, layer 6 was the most densely innervated layer of orbitofrontal areas 13 and 11, and frontal polar area 10. Areas V24 and O25 showed a unique innervation of their middle layers, including layer 4. Areas OPAll, OPro, and M25 also had high densities of boutons in their middle layers, though they lack, or have a poorly developed, layer 4. Layer 3, in general, was sparsely innervated and no area of the prefrontal cortex included a predominant distribution of boutons in layer 3. However, in areas OPro, OPAll, M25 and to a lesser extent in area 24, significant densities of labeled boutons were noted in layer 3 (Fig. 6D).

We then pooled laminar data to determine the relative density of boutons in superficial (1−3) and deep (4−6) layers across areas, as shown in Figure 6E. In most areas the percentage of axonal terminals in superficial layers exceeded the deep, particularly in agranular (MPAll, OPAll) and dysgranular (D24, M25 and OPro) cortices (Fig. 6E). In other dysgranular and eulaminate cortices, the density of axonal terminals was nearly equal in the superficial and deep layers. The proportion of axonal terminals in the deep layers was slightly higher than the superficial in only a few areas, including orbitofrontal areas 11 and 12 (Fig. 6E).

Comparison of the input and output zones of prefrontal cortices connected with the amygdala

We next compared the relative density of projection neurons to axonal terminals in prefrontal cortices connected with the amygdala. The goal was to determine the extent to which prefrontal areas were predominantly receivers of input from the amygdala, or senders of projections to the amygdala. This was accomplished using normalized data, by expressing the estimated number of boutons for each area as a percentage of the sum of boutons in all prefrontal areas (Fig. 8), and by applying an analogous normalization to the number of projection neurons found in prefrontal areas. In some prefrontal areas the percentage of input from the amygdala significantly exceeded the percentage of output from the same area to the amygdala (Figs. 8A-C, E, F, green coded, I > O). Of the heavily innervated caudal medial prefrontal areas, this category included area MPAll (Fig. 8A, D-F). The medial parts of areas 9 (M9) and 10 (M10) also belonged to the category I > O, as did lateral areas 8, dorsal area 46 (D46), and D9, but the density of amygdalar innervation was substantially lower. Caudal orbitofrontal areas OPAll, OPro, O25, and 13 also belonged to the category I > O, although the differences in percentages of input and output were not significant (Figs. 8C,D-F). The second pattern included prefrontal cortices with significantly higher proportion of output compared to input

(Figs. 8A-C, E, F, red coded, O > I), and included caudal medial areas 24, M25, and 32, and all rostrally situated orbitofrontal areas (11, O14, O12, and 10). On the lateral surface, areas dorsal 10 (D10), L12, and V46 were in the category O > I. These findings are summarized in Fig. 8E,F. Figure 8F takes into account the overall density of connections, showing prefrontal areas possessing particularly strong links with the amygdala towards the top of the diagram, and also indicates the input-output characteristics of areas. 'Senders' (projecting more strongly to, than receiving projections from, the amygdala) are on the left and 'receivers' (showing the opposite balance of projections) are shown on the right of the figure.

We then investigated the input and output connections for the superficial and deep layers of prefrontal cortices and the results are summarized in Figure 9A, B. By analogy with sensory corticocortical connections, projection neurons from the superficial layers (2−3) in prefrontal cortices directed to the amygdala may be considered 'feedforward', and axonal terminations from the amygdala terminating in the upper layers (1-upper 3) of prefrontal cortices may be considered 'feedback'. Only a few prefrontal areas showed a balanced form of this pattern, and included caudal areas D24, M25, and OPro (Fig. 9A,B). Interestingly, feedback input from the amygdala in the superficial layers was widespread and included most medial and orbitofrontal areas (Fig. 9A). Medial area MPAll was distinguished for receiving substantial feedback input from the amygdala but not reciprocating with a significant output to the amygdala. Feedforward input from the amygdala to the middle layers of prefrontal cortex, and feedback output from the deep layers of prefrontal cortex was more widespread and included nearly all medial and orbitofrontal cortices. Areas that received a relatively high proportion of feedforward input from the amygdala into their middle layers included the caudally situated medial and orbitofrontal cortices (areas MPAll, M25, OPAll, OPro, and 13; Fig. 9B). Feedback output from the prefrontal cortices, however, was not as evenly distributed. Areas D24 and M25 included a significantly high percentage of feedback output among prefrontal areas (Fig. 9B). Nearly all orbitofrontal areas as well as lateral area 12 provided substantial feedback projections to the amygdala. A population analysis of the relationship of 'feedforward' prefrontal projection neurons from layers 2−3 to 'feedback' terminations from the amygdala in prefrontal layers 1- upper 3 revealed a significant correlation (r=0.60, P=0.003; Fig. 9C). In Figure 9C, for example, the placement of area V24 indicates that 29% of its projection neurons directed to the amygdala (shown on x-axis) originated from layers 2 and 3, and the complementary 71% from layers 5 and 6 (not shown), while 57% of the amygdalar terminations in area V24 (shown on y-axis) were found in layers 1 through 3, and the remaining 43% in layers 4 through 6 (not shown).

The relationship of amygdalar connections to neurochemical classes of inhibitory neurons in prefrontal cortices

An important component of cortical circuits is their relationship with GABAergic interneurons. We addressed this issue by determining the relationship of prefrontal connections with the amygdala to two neurochemical classes of local inhibitory neurons that are positive for the calcium binding proteins CB and PV. These neurochemical classes of inhibitory neurons have a distinct laminar distribution in prefrontal cortices (Gabbott and Bacon, 1996;Dombrowski et al., 2001). We conducted a quantitative analysis to determine the number of CB and PV interneurons within a 75 μm radius from labeled projection neurons in four cases with BDA injection in the amygdala (cases BBr; BDr; BBl; BDl; Table 1). In medial areas D24, and M25, and orbitofrontal areas OPAll, and OPro more CB interneurons surrounded projection neurons directed to the amygdala than did PV interneurons. Combined, these prefrontal areas included the largest percentage (~ 50%) of projection neurons directed to the amygdala. Other medial and orbitofrontal areas included equal numbers of CB and PV interneurons associated with each projection neuron (areas V24, 13, and O25).

Examples of the relationship of prefrontal CB and PV interneurons to prefrontal connections with the amygdala are shown in Figure 10. Caudal medial and orbitofrontal areas included higher associations with CB than PV interneurons (areas D24, M25, OPAll, and OPro). Areas V24 and L12, both biased ‘senders’ of projections, were unique among prefrontal areas by having on average more PV positive interneurons surrounding each projection neuron directed to the amygdala than other medial and orbitofrontal areas. These two areas together provided approximately 12% of projection neurons directed to the amygdala, substantially fewer than areas where projection neurons were strongly associated with CB interneurons. The few projection neurons found in lateral prefrontal cortices, other than area L12, were mostly surrounded by PV interneurons, and contributed about 6% of the projection neurons to the amygdala.

Axonal terminals from the amygdala overlapped largely with CB interneurons in layers 2 and upper 3, where CB interneurons predominate (Fig. 10A). The axonal terminals from the amygdala in some prefrontal areas also targeted the PV-dominated middle layers, although their densities were substantially lower (Fig. 10D).

Discussion

Caudal orbitofrontal and anterior cingulate areas had the strongest connections with the amygdala, confirming previous studies (Porrino et al., 1981;Amaral and Price, 1984). The present findings further indicate that prefrontal connections with the amygdala were more extensive than previously thought, extending beyond the most heavily linked orbitofrontal and medial cingulate cortices, described previously for primates and rats (Nauta, 1961;Jacobson and Trojanowski, 1975;Porrino et al., 1981;Amaral and Price, 1984;Cassell et al., 1989;Barbas and De Olmos, 1990;Morecraft et al., 1992;Carmichael and Price, 1995). Unprecedented quantitative analysis of prefrontal connections with the amygdala revealed marked regional differences in their density, laminar organization, and input-output relationships, as summarized in Figure 11.

Regional specificity in the density and pattern of prefrontal connections with the amygdala

All prefrontal areas were connected with the amygdala, but their connection density varied widely. At one extreme, area 10 had the lowest density of connections. At the other extreme, posterior orbitofrontal and anterior cingulate areas had the densest connections, accounting for about half of all prefrontal projection neurons directed to the amygdala, and receiving projections from the amygdala reaching levels of 1−6 million boutons per mm^3 in the most heavily targeted layers 1 and 2.

Widespread 'feedback' and focal 'feedforward' laminar patterns—The most common projection from prefrontal areas to the amygdala originated in the upper part of layer 5, and the reciprocal projections terminated widely in two bands in prefrontal cortices, one innervating layers 1 and 2, and another innervating layers 5−6, consistent with previous findings (Porrino et al., 1981;Amaral and Price, 1984). In addition, in several posterior orbitofrontal and anterior cingulate areas axons from the amygdala innervated the middle layers, or terminated in columns spanning the width of the cortex, in patterns that eluded previous qualitative observations. In turn, anterior cingulate and caudal orbitofrontal cortices issued projections to the amygdala from layer 5 as well as layer 3.

Are these complex laminar patterns consistent with rules that underlie corticocortical connections? Our analysis revealed that the laminar patterns of input to output connections were significantly correlated (Fig. 9C). Thus, the higher the proportion of output from 'feedforward' layer 3, the higher also the ‘feedback’ input to the upper layers, comparable to reciprocal corticocortical connections. This trend provides novel evidence that prefrontal

connections with the amygdala follow rules similar to corticocortical connections, including more widespread feedback connections in both directions.

Sequence of information processing for emotions

The sequence of information processing is known with certainty only in early processing sensory areas from functional studies. The laminar patterns of connections linking sensory areas have been used to categorize pathways as 'feedforward' if they target mostly the middle layers, 'feedback' if they avoid the middle layers, and 'lateral' when they target all layers [reviewed in (Felleman and Van Essen, 1991)]. These general patterns provide a handle for interpreting connections between high-order association areas, where the sequence of information processing is unknown. The prefrontal cortex is a prime example of such a region, and also has a fundamental role in tasks with sequential components [e.g., (Heidbreder and Groenewegen, 2003)].

The three connection categories, however, do not sufficiently account for the large variety of laminar patterns of connections. Another model provides a different perspective to categorical description of pathways, based on the graded laminar patterns of connections seen in all cortical systems (Barbas, 1986). This model posits that the relative laminar density of corticocortical connections depends on the structural relationship of the linked areas, where structure is defined by the number of layers and overall neuronal density that characterize different types of cortices (Barbas and Rempel-Clower, 1997;Dombrowski et al., 2001). Thus, when two areas with non-equivalent structure are linked (i.e., A and B), projection neurons are found mostly in the deep layers (5−6) of the area with fewer layers or lower cell density (area A), and their axons terminate in the superficial layers (especially layer 1) of the cortex with more layers or higher cell density (area B). In the reverse direction, projection neurons are found in the superficial layers (layers 2−3, of area B) and their axons terminate in the middle-deep layers (especially bottom of layer 3-upper layer 5 of area A). Moreover, the structural model is relational, that is, the distribution of connections is proportional to the relative difference in laminar structure between the linked areas [e.g., (Barbas and Rempel-Clower, 1997;Barbas et al., 1999;Rempel-Clower and Barbas, 2000;Barbas et al., 2005a;Medalla and Barbas, 2006)]. We now apply the structural model to prefrontal connections with the amygdala. The significance of determining the laminar specificity of connections is based on evidence that pathways function within laminar microenvironments that differ vastly in neurochemical, inhibitory, and synaptic features [e.g., (Barbas et al., 2005b;Germuska et al., 2006;Medalla and Barbas, 2006)].

Common feedback connections—The most common projections from prefrontal cortices to the amygdala originating in layer 5 resemble other cortico-subcortical projections, like those directed to the caudate, brainstem, some thalamic nuclei [e.g. (Arikuni and Kubota, 1986;Xiao and Barbas, 2004)], and corticocortical feedback projections. Interestingly, the ubiquitous two-band termination of axons from the amygdala, which avoided the middle cortical layers, also resembles corticocortical feedback projections. In densely innervated prefrontal areas, axonal terminations from the amygdala stretched expansively in bands of 2 −5 mm parallel to the pial surface, where they encounter the dendrites of neurons from other layers. Projections to layer 1 from the thalamus (Jones, 1998) depolarize extensive fields in the upper cortical layers [e.g., (Roland, 2002)], and may have a similar function here.

The massive terminations from the amygdala in cortical layers 1 and 2 intermingled with the distinct neurochemical class of calbindin positive inhibitory neurons, whose activity has been associated with focusing attention on relevant features and suppressing distractors (Wang et al., 2004). This widespread pathway from the amygdala to prefrontal cortices may have a prominent role in focusing attention on motivationally relevant stimuli, consistent with the role

of the amygdala in emotional alertness and vigilance [reviewed in (Gallagher and Holland, 1994;LeDoux, 2000;Davis and Whalen, 2001;Zald, 2003)].

Focal feedforward projections—Axonal terminations from the amygdala innervated to a significant extent the middle layers of caudal orbitofrontal and anterior cingulate areas as well. What type of information does the amygdala convey to these areas? To begin to address this issue we consider the rich cortical sensory input to the amygdala from all modalities [reviewed in (Barbas et al., 2002)], which terminates in the same parts of the amygdala that project to the posterior orbitofrontal cortex (Barbas and De Olmos, 1990;Ghashghaei and Barbas, 2002). Based on the key role of the amygdala in affective behavior [reviewed in (Damasio, 1994;Gallagher and Holland, 1994;LeDoux, 2000)], its feedforward projections to orbitofrontal cortex may convey the affective significance of external sensory stimuli, consistent with the involvement of orbitofrontal cortex in rapid perception and reward contingencies [e.g., (Rolls, 1996;Tremblay and Schultz, 1999;Bar et al., 2006)].

In the opposite direction, an unusual projection to the amygdala originated in cortical layer 3, and emanated in significant numbers only from posterior orbitofrontal and anterior cingulate areas. What type of information do these areas send to the amygdala in a feedforward manner? Posterior orbitofrontal and cingulate cortices receive robust projections from cortical and subcortical limbic structures [reviewed in (Barbas et al., 2002)], and may relay information to the amygdala about the internal milieu, including internalized emotions, such as jealousy, embarrassment and guilt, which evoke emotional arousal.

Complementary circuits through prefrontal cortices and the amygdala for emotional-cognitive processing—Our findings further suggest specialization in the connections of anterior cingulate versus orbitofrontal cortices with the amygdala. Anterior cingulate areas sent proportionally more projections to the amygdala than they received, and also have stronger connections with central autonomic structures (Neafsey, 1990;Alheid and Heimer, 1996;Barbas et al., 2003;Vertes, 2004) than the orbitofrontal. Based on these features, anterior cingulate areas may be considered more ‘senders' than 'receivers' in the terminology of Kötter and Stephan (Kötter and Stephan, 2003), consistent with their role in affective vocalization in primates, and extinction of fear in rats [reviewed in (Vogt and Barbas, 1988;Devinsky et al., 1995;Davis et al., 1997;Heidbreder and Groenewegen, 2003)].

Posterior orbitofrontal cortices, on the other hand, are unique among prefrontal areas for having partly segregated input and output connections in the amygdala (Ghashghaei and Barbas, 2002). Moreover, posterior orbitofrontal areas target dual systems in the amygdala that can potentially increase or decrease autonomic drive, activated perhaps according to the emotional significance of the situation or environment (Ghashghaei and Barbas, 2002;Barbas et al., 2003;Arana et al., 2003;Sugase-Miyamoto and Richmond, 2005;Wellman et al., 2005;Paton et al., 2006).

Decision for action based on the significance of the environment is a complex process that likely involves many structures, including communication between caudal lateral prefrontal cortices, which are thought to have executive functions, and orbitofrontal and medial prefrontal cortices associated with processing the value of stimuli [(Wallis and Miller, 2003;Padoa-Schioppa and Assad, 2006); reviewed in (Miller and Cohen, 2001)]. Transmission of signals from orbitofrontal and medial prefrontal cortices pertaining to the value of stimuli may be conveyed to the upper layers of lateral prefrontal areas, according to the rules of the structural model. In turn, when lateral prefrontal areas project to orbitofrontal cortices, they target the middle layers, including layer 5 (Barbas and Rempel-Clower, 1997), which is the chief output layer to the amygdala, as shown here and in previous studies [e.g., (Aggleton et al., 1980)]. This interaction between orbitofrontal and lateral prefrontal cortices would appear to be

necessary, since lateral prefrontal areas have limited output to the amygdala. Collaborative signals are thus transmitted along laminar-specific pathways suggesting sequential flow of signals pertinent to emotional and cognitive processes.

Psychiatric diseases associated with the prefrontal cortices and the amygdala are many and varied, including obsessive-compulsive disorder, panic disorder, post-traumatic stress disorder, depression and autism [e.g., (Rauch et al., 2000;Hariri et al., 2003;Mayberg, 2003;Drevets, 2003;Kent et al., 2005;Bachevalier and Loveland, 2006;Williams et al., 2006)]. Pathology at different nodes of this elaborate but orderly system may underlie the varied symptomatology in these diseases.

ACKNOWLEDGMENTS

We thank Dr. Ron Killiany for help with brain imaging and Ms. Karen Trait for technical assistance. Research was supported by NIH grants from NIMH and NINDS.

References

Aggleton JP, Burton MJ, Passingham RE. Cortical and subcortical afferents to the amygdala of the rhesus monkey (*Macaca mulatta*). Brain Research 1980;190:347–368. [PubMed: 6768425]

Alheid GF, Heimer L. Theories of basal forebrain organization and the “emotional motor system”. Progress in Brain Research 1996;107:461–484. [PubMed: 8782537]

Amaral DG, Price JL. Amygdalo-cortical projections in the monkey *(Macaca fascicularis)*. Journal of Comparative Neurology 1984;230:465–496. [PubMed: 6520247]

Arana FS, Parkinson JA, Hinton E, Holland AJ, Owen AM, Roberts AC. Dissociable contributions of the human amygdala and orbitofrontal cortex to incentive motivation and goal selection. J Neurosci 2003;23:9632–9638. [PubMed: 14573543]

Arikuni T, Kubota K. The organization of prefrontocaudate projections and their laminar origin in the Macaque monkey: A retrograde study using HRP-Gel. Journal of Comparative Neurology 1986;244:492–510. [PubMed: 2420836]

Bachevalier J, Loveland KA. The orbitofrontal-amygdala circuit and self-regulation of social-emotional behavior in autism. Neuroscience & Biobehavioral Reviews 2006;30:97–117. [PubMed: 16157377]

Bacon SJ, Headlam AJ, Gabbott PL, Smith AD. Amygdala input to medial prefrontal cortex (mPFC) in the rat: a light and electron microscope study. Brain Reserch 1996;720:211–219.

Bar M, Kassam KS, Ghuman AS, Boshyan J, Schmid AM, Dale AM, Hamalainen MS, Marinkovic K, Schacter DL, Rosen BR, Halgren E. Top-down facilitation of visual recognition. Proc Natl.Acad.Sci.U.S.A 2006;103:449–454. [PubMed: 16407167]

Barbas H. Pattern in the laminar origin of corticocortical connections. Journal of Comparative Neurology 1986;252:415–422. [PubMed: 3793985]

Barbas H. Connections underlying the synthesis of cognition, memory, and emotion in primate prefrontal cortices. Brain Research Bulletin 2000;52:319–330. [PubMed: 10922509]

Barbas H, De Olmos J. Projections from the amygdala to basoventral and mediodorsal prefrontal regions in the rhesus monkey. Journal of Comparative Neurology 1990;301:1–23. [PubMed: 1706353]

Barbas H, Ghashghaei H, Dombrowski SM, Rempel-Clower NL. Medial prefrontal cortices are unified by common connections with superior temporal cortices and distinguished by input from memory-related areas in the rhesus monkey. Journal of Comparative Neurology 1999;410:343–367. [PubMed: 10404405]

Barbas, H.; Ghashghaei, H.; Rempel-Clower, N.; Xiao, D. Anatomic basis of functional specialization in prefrontal cortices in primates. In: Grafman, J., editor. Handbook of Neuropsychology. 2 ed.. Elsevier Science B.V.; Amsterdam: 2002. p. 1-27.

Barbas H, Hilgetag CC, Saha S, Dermon CR, Suski JL. Parallel organization of contralateral and ipsilateral prefrontal cortical projections in the rhesus monkey. BMC.Neurosci 2005a;6:32. [PubMed: 15869709]

Barbas H, Medalla M, Alade O, Suski J, Zikopoulos B, Lera P. Relationship of prefrontal connections to inhibitory systems in superior temporal areas in the rhesus monkey. Cerebral Cortex 2005b; 15:1356–1370. [PubMed: 15635060]

Barbas H, Pandya DN. Architecture and intrinsic connections of the prefrontal cortex in the rhesus monkey. Journal of Comparative Neurology 1989;286:353–375. [PubMed: 2768563]

Barbas H, Rempel-Clower N. Cortical structure predicts the pattern of corticocortical connections. Cerebral Cortex 1997;7:635–646. [PubMed: 9373019]

Barbas H, Saha S, Rempel-Clower N, Ghashghaei T. Serial pathways from primate prefrontal cortex to autonomic areas may influence emotional expression. BMC.Neurosci 2003;4:25. [PubMed: 14536022]

Bechara A, Damasio H, Damasio AR. Emotion, decision making and the orbitofrontal cortex. Cerebral Cortex 2000;10:295–307. [PubMed: 10731224]

Bechara A, Damasio H, Tranel D, Damasio AR. Deciding advantageously before knowing the advantageous strategy. Science 1997;275:1293–1295. [PubMed: 9036851]

Carmichael ST, Price JL. Limbic connections of the orbital and medial prefrontal cortex in macaque monkeys. Journal of Comparative Neurology 1995;363:615–641. [PubMed: 8847421]

Cassell MD, Chittick CA, Siegel MA, Wright DJ. Collateralization of the amygdaloid projections of the rat prelimbic and infralimbic cortices. Journal of Comparative Neurology 1989;279:235–248. [PubMed: 2913068]

Damasio, AR. Descarte's Error: Emotion, Reason, and the Human Brain. 1 ed.. G. P. Putnam's Sons; New York: 1994.

Davis M, Walker DL, Lee Y. Amygdala and bed nucleus of the stria terminalis: differential roles in fear and anxiety measured with the acoustic startle reflex. Philos.Trans.R.Soc.Lond B Biol.Sci 1997;352:1675–1687. [PubMed: 9415919]

Davis M, Whalen PJ. The amygdala: vigilance and emotion. Mol.Psychiatry 2001;6:13–34. [PubMed: 11244481]

De Olmos, J. Amygdaloid nuclear gray complex. In: Paxinos, G., editor. The Human Nervous System. Acedemic Press, Inc.; San Diego: 1990. p. 583-710.

Devinsky O, Morrell MJ, Vogt BA. Contributions of anterior cingulate cortex to behaviour. Brain 1995;118:279–306. [PubMed: 7895011]

Dombrowski SM, Hilgetag CC, Barbas H. Quantitative architecture distinguishes prefrontal cortical systems in the rhesus monkey. Cerebral Cortex 2001;11:975–988. [PubMed: 11549620]

Drevets WC. Neuroimaging abnormalities in the amygdala in mood disorders. Annals of the New York Academy of Sciences 2003;985:420–444. [PubMed: 12724175]

Felleman DJ, Van Essen DC. Distributed hierarchical processing in the primate cerebral cortex. Cerebral Cortex 1991;1:1–47. [PubMed: 1822724]

Fuster JM. Executive frontal functions. Experimental Brain Research 2000;133:66–70.

Gabbott PL, Bacon SJ. Local circuit neurons in the medial prefrontal cortex (areas 24a,b,c, 25 and 32) in the monkey: II. Quantitative areal and laminar distributions. Journal of Comparative Neurology 1996;364:609–636. [PubMed: 8821450]

Gallagher M, Holland PC. The amygdala complex: multiple roles in associative learning and attention. Proceedings of the National Academy of Sciences of the United States of America 1994;91:11771–11776. [PubMed: 7991534]

Germuska M, Saha S, Fiala J, Barbas H. Synaptic distinction of laminar specific prefrontal-temporal pathways in primates. Cerebral Cortex 2006;16:865–875. [PubMed: 16151179]

Ghashghaei HT, Barbas H. Pathways for emotions: Interactions of prefrontal and anterior temporal pathways in the amygdala of the rhesus monkey. Neuroscience 2002;115:1261–1279. [PubMed: 12453496]

Gundersen HJG, Bagger P, Bendtsen TF, Evans SM, Korbo L, Marcussen N, Moller A, Nielsen K, Nyengaard JR, Pakkenberg B, Sorensen FB, Vesterby A, West MJ. The new stereological tools: disector, fractionator, nucleator and point sample intercepts and their use in pathological research and diagnosis. Acta Pathologica,Microbiologica et Immunologica Scandinavica 1988;96:857–881.

Hariri AR, Mattay VS, Tessitore A, Fera F, Weinberger DR. Neocortical modulation of the amygdala response to fearful stimuli. Biological Psychiatry 2003;53:494–501. [PubMed: 12644354]

Heidbreder CA, Groenewegen HJ. The medial prefrontal cortex in the rat: evidence for a dorso-ventral distinction based upon functional and anatomical characteristics. Neuroscience & Biobehavioral Reviews 2003;27:555–579. [PubMed: 14599436]

Izquierdo A, Murray EA. Opposing effects of amygdala and orbital prefrontal cortex lesions on the extinction of instrumental responding in macaque monkeys. Eur.J Neurosci 2005;22:2341–2346. [PubMed: 16262672]

Jacobson S, Trojanowski JQ. Amygdaloid projections to prefrontal granular cortex in rhesus monkey demonstrated with horseradish peroxidase. Brain Research 1975;100:132–139. [PubMed: 810217]

Jones EG. A new view of specific and nonspecific thalamocortical connections. Advances in Neurology 1998;77:49–71. [PubMed: 9709817]

Kent JM, Coplan JD, Mawlawi O, Martinez JM, Browne ST, Slifstein M, Martinez D, Abi-Dargham A, Laruelle M, Gorman JM. Prediction of panic response to a respiratory stimulant by reduced orbitofrontal cerebral blood flow in panic disorder. Am J Psychiatry 2005;162:1379–1381. [PubMed: 15994724]

Kötter R, Stephan KE. Network participation indices: characterizing component roles for information processing in neural networks. Neural Networks 2003;16:1261–1275. [PubMed: 14622883]

LeDoux JE. Emotion circuits in the brain. Annual Review of Neuroscience 2000;23:155–184.

Levy R, Goldman-Rakic PS. Segregation of working memory functions within the dorsolateral prefrontal cortex. Experimental Brain Research 2000;133:23–32.

Mayberg HS. Modulating dysfunctional limbic-cortical circuits in depression: towards development of brain-based algorithms for diagnosis and optimised treatment. British Medical Bulletin 2003;65:193–207. [PubMed: 12697626]

Medalla M, Barbas H. Diversity of laminar connections linking periarcuate and lateral intraparietal areas depends on cortical structure. Eur.J Neurosci 2006;23:161–179. [PubMed: 16420426]

Miller EK, Cohen JD. An integrative theory of prefrontal cortex function. Annu.Rev.Neurosci 2001;24:167–202. [PubMed: 11283309]

Morecraft RJ, Geula C, Mesulam M-M. Cytoarchitecture and neural afferents of orbitofrontal cortex in the brain of the monkey. Journal of Comparative Neurology 1992;323:341–358. [PubMed: 1460107]

Nauta WJH. Fibre degeneration following lesions of the amygdaloid complex in the monkey. Journal of Anatomy 1961;95:515–531. [PubMed: 14478601]

Neafsey EJ. Prefrontal cortical control of the autonomic nervous system: Anatomical and physiological observations. Progress in Brain Research 1990;85:147–166. [PubMed: 2094892]

Ottersen OP. Connections of the amygdala of the rat IV: corticoamygdaloid and intraamygdaloid connections as studied with axonal transport of horseradish peroxidase. Journal of Comparative Neurology 1982;205:30–48. [PubMed: 7068948]

Padoa-Schioppa C, Assad JA. Neurons in the orbitofrontal cortex encode economic value. Nature 2006;441:223–226. [PubMed: 16633341]

Pandya DN, Van Hoesen GW, Domesick VB. A cingulo-amygdaloid projection in the rhesus monkey. Brain Reserch 1973;61:369–373.

Paton JJ, Belova MA, Morrison SE, Salzman CD. The primate amygdala represents the positive and negative value of visual stimuli during learning. Nature 2006;439:865–870. [PubMed: 16482160]

Petrides M. Specialized systems for the processing of mnemonic information within the primate frontal cortex. Philosophical Transactions of the Royal Society of London.Series B: Biological Sciences 1996;351:1455–1462.

Porrino LJ, Crane AM, Goldman-Rakic PS. Direct and indirect pathways from the amygdala to the frontal lobe in rhesus monkeys. Journal of Comparative Neurology 1981;198:121–136. [PubMed: 6164704]

Price, JL.; Russchen, FT.; Amaral, DG. The limbic region. II. The amygdaloid complex. In: Björklund, A.; Hökfelt, T.; Swanson, LW., editors. Handbook of Chemical Neuroanatomy. Vol.5, Integrated Systems of the CNS, Part I. Elsevier, Amsterdam: 1987. p. 279-381.

Rauch SL, Whalen PJ, Shin LM, McInerney SC, Macklin ML, Lasko NB, Orr SP, Pitman RK. Exaggerated amygdala response to masked facial stimuli in posttraumatic stress disorder: a functional MRI study. Biological Psychiatry 2000;47:769–776. [PubMed: 10812035]

Reiner A, Veenman CL, Medina L, Jiao Y, Del Mar N, Honig MG. Pathway tracing using biotinylated dextran amines. J Neurosci.Methods 2000;103:23–37. [PubMed: 11074093]

Rempel-Clower NL, Barbas H. The laminar pattern of connections between prefrontal and anterior temporal cortices in the rhesus monkey is related to cortical structure and function. Cerebral Cortex 2000;10:851–865. [PubMed: 10982746]

Roberts AC, Wallis JD. Inhibitory control and affective processing in the prefrontal cortex: neuropsychological studies in the common marmoset. Cerebral Cortex 2000;10:252–262. [PubMed: 10731220]

Roland PE. Dynamic depolarization fields in the cerebral cortex. Trends in Neuroscience 2002;25:183–190.

Rolls ET. The orbitofrontal cortex. Philosophical Transactions of the Royal Society of London.Series B: Biological Sciences 1996;351:1433–143.

Russchen FT. Amygdalopetal projections in the cat. I. Cortical afferent connections. A study with retrograde and anterograde tracing techniques. J Comp Neurol 1982;206:159–179. [PubMed: 7085926]

Schoenbaum G, Chiba AA, Gallagher M. Orbitofrontal cortex and basolateral amygdala encode expected outcomes during learning. Nature Neuroscience 1998;1:155–159.

Schoenbaum G, Chiba AA, Gallagher M. Changes in functional connectivity in orbitofrontal cortex and basolateral amygdala during learning and reversal training. Journal of Neuroscience 2000;20:5179–5189. [PubMed: 10864975]

Stefanacci L, Suzuki WA, Amaral DG. Organization of connections between the amygdaloid complex and the perirhinal and parahippocampal cortices in macaque monkeys. Journal of Comparative Neurology 1996;375:552–582. [PubMed: 8930786]

Sugase-Miyamoto Y, Richmond BJ. Neuronal signals in the monkey basolateral amygdala during reward schedules. J Neurosci 2005;25:11071–11083. [PubMed: 16319307]

Tremblay L, Schultz W. Relative reward preference in primate orbitofrontal cortex. Nature 1999;398:704–708. [PubMed: 10227292]

Van Hoesen, GW. The differential distribution, diversity and sprouting of cortical projections to the amygdala of the rhesus monkey. In: Ben-Ari, Y., editor. The Amygdaloid complex. Elsevier/North Holland Biomedical Press; Amsterdam: 1981. p. 77-90.

Veenman CL, Reiner A, Honig MG. Biotinylated dextran amine as an anterograde tracer for single- and double-labeling studies. J.Neurosci.Methods 1992;41:239–254. [PubMed: 1381034]

Vertes RP. Differential projections of the infralimbic and prelimbic cortex in the rat. Synapse 2004;51:32–58. [PubMed: 14579424]

Vogt, BA.; Barbas, H. Structure and connections of the cingulate vocalization region in the rhesus monkey. In: Newman, JD., editor. The Physiological control of mammalian vocalization. Plenum Publ. Corp.; New York: 1988. p. 203-225.

Wallis JD, Miller EK. Neuronal activity in primate dorsolateral and orbital prefrontal cortex during performance of a reward preference task. Eur.J Neurosci 2003;18:2069–2081. [PubMed: 14622240]

Wang XJ, Tegner J, Constantinidis C, Goldman-Rakic PS. Division of labor among distinct subtypes of inhibitory neurons in a cortical microcircuit of working memory. Proc.Natl.Acad.Sci.U.S.A 2004;101:1368–1373. [PubMed: 14742867]

Wellman LL, Gale K, Malkova L. GABAA-mediated inhibition of basolateral amygdala blocks reward devaluation in macaques. J Neurosci 2005;25:4577–4586. [PubMed: 15872105]

West MJ, Gundersen HJG. Unbiased stereological estimation of the number of neurons in the human hippocampus. Journal of Comparative Neurology 1990;296:1–22. [PubMed: 2358525]

Williams LM, Kemp AH, Felmingham K, Barton M, Olivieri G, Peduto A, Gordon E, Bryant RA. Trauma modulates amygdala and medial prefrontal responses to consciously attended fear. Neuroimage 2006;29:347–357. [PubMed: 16216534]

Williams RW, Rakic P. Three-dimensional counting: An accurate and direct method to estimate numbers of cells in sectioned material. Journal of Comparative Neurology 1988;278:344–352. [PubMed: 3216047]

Xiao D, Barbas H. Circuits through prefrontal cortex, basal ganglia, and ventral anterior nucleus map pathways beyond motor control. Thalamus & Related Systems 2004;2:325–343.

Zald DH. The human amygdala and the emotional evaluation of sensory stimuli. Brain Res Brain Res Rev 2003;41:88–123. [PubMed: 12505650]

Zikopoulos B, Barbas H. Prefrontal projections to the thalamic reticular nucleus form a unique circuit for attentional mechanisms. Journal of Neuroscience 2006;26:7348–7361. [PubMed: 16837581]

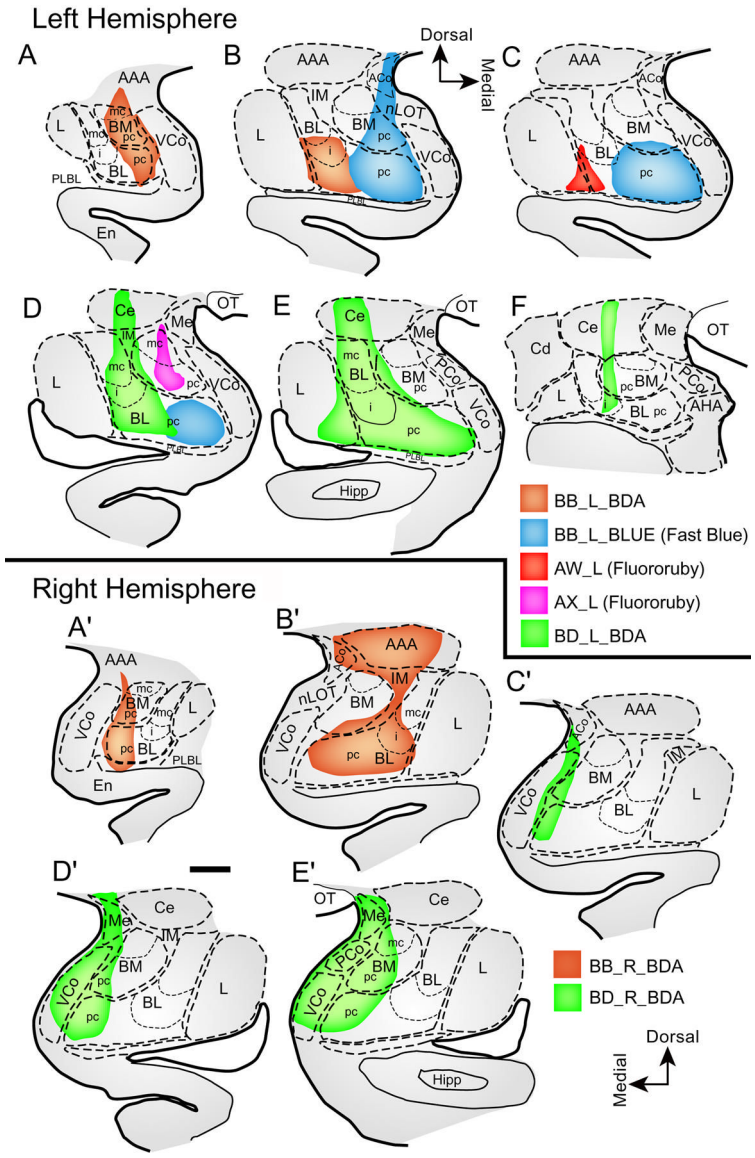

Figure 1. Composite of the injection sites in the amygdala

A-F, Diagrams of coronal sections through rostral (A) to caudal (F) levels of the amygdala showing a composite of the injection sites in the left hemisphere.***A'-E'*** Diagrams of coronal sections through rostral (A') to caudal (E') levels of the amygdala showing the injection sites in the right hemisphere. Color key shows the corresponding cases. Scale bar, 1 mm. Abbreviations: AAA, anterior amygdalar area; ACo, anterior cortical nucleus; AHA, amygdalo-hippocampal area; BM, basomedial nucleus (also known as accessory basal); BL, basolateral nucleus; Cd, caudate; Ce, central nucleus; En, Entorhinal cortex; Hipp, hippocampus; IM, intercalated masses; L, lateral nucleus; Me, medial nucleus; nLOT, nucleus of the lateral olfactory tract; OT, optic tract; PCo, posterior cortical nucleus; PLBL, paralamellar basolateral; VCo, ventral cortical nucleus; mc, magnocellular; pc, parvicellular sectors of BM or BL nuclei; i, intermediate sector of BL.

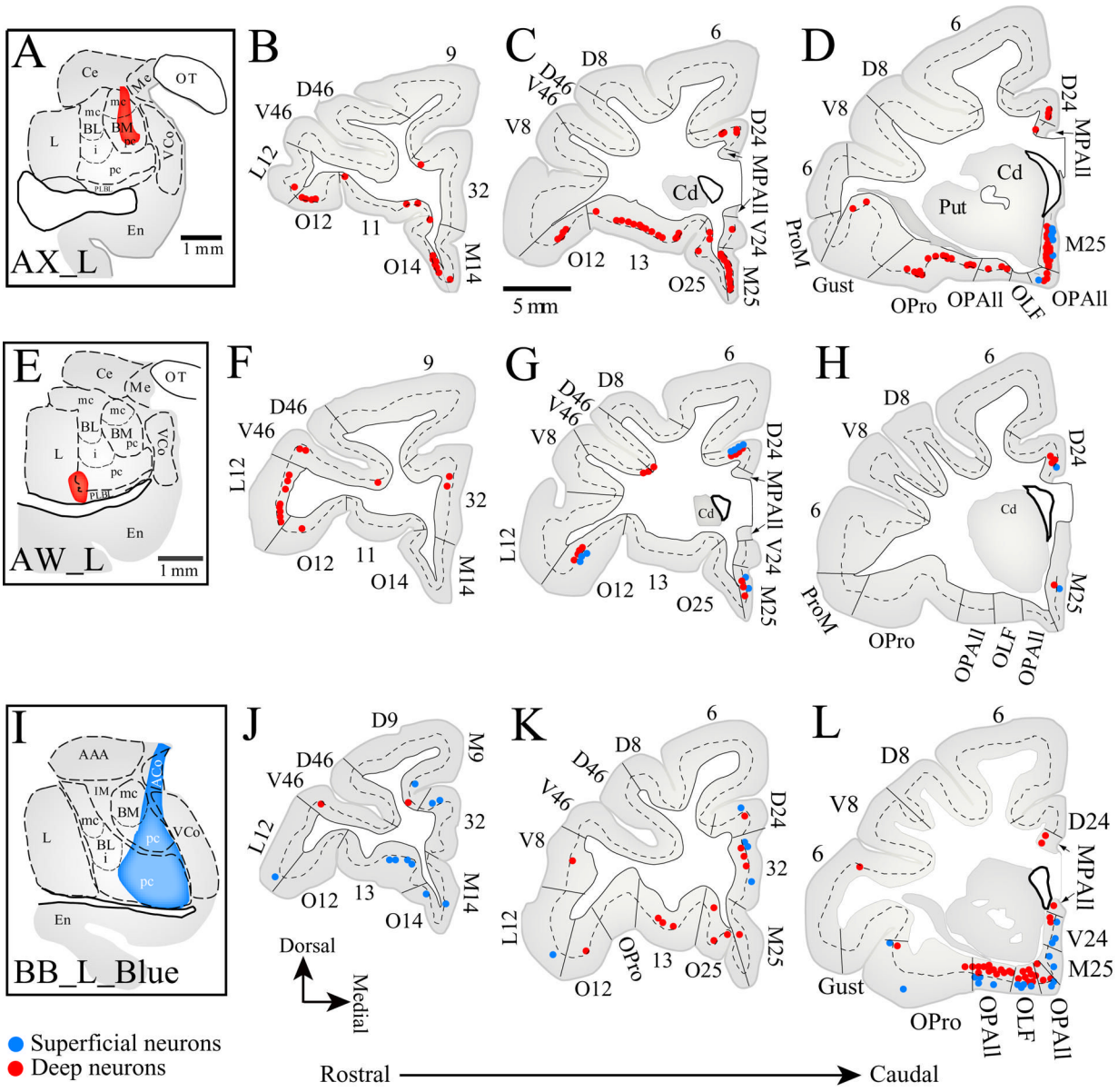

Figure 2. Origin of projection neurons directed to the amygdala from the prefrontal cortices in three cases

Distribution of labeled neurons in the deep (red dots) and superficial (blue dots) layers in coronal sections of rostral (B) to caudal (D) prefrontal cortices mapped after injection of retrograde tracers in the amygdala. ***Top***, The injection of the retrograde tracer fluororuby was in the ventral part of BMpc and BMmc nuclei (A, red area; Case AX). ***Center***, The injection of the retrograde tracer fluororuby was in the ventral part of BLpc and L nuclei (A, red area; case AW). ***Bottom***, The injection of the retrograde tracer fast blue was in BLpc, BMpc, and ACo nuclei, and nLOT (A, blue area; Case BBb). The dotted line through the cortex shows the upper border of layer 5. Small font letters and numbers in coronal sections refer to architectonic areas separated by slanted lines. Letters before cortical architectonic areas refer to: D, dorsal; M, medial; O, orbital; V, ventral. Other abbreviations: Cd, caudate; Gust, gustatory; MPAll, medial periallocortex; OLF, olfactory; OPAll, orbital periallocortex; OPro, orbital

proisocortex; Put, putamen; These conventions also apply for other figures depicting cortical areas or subcortical structures.

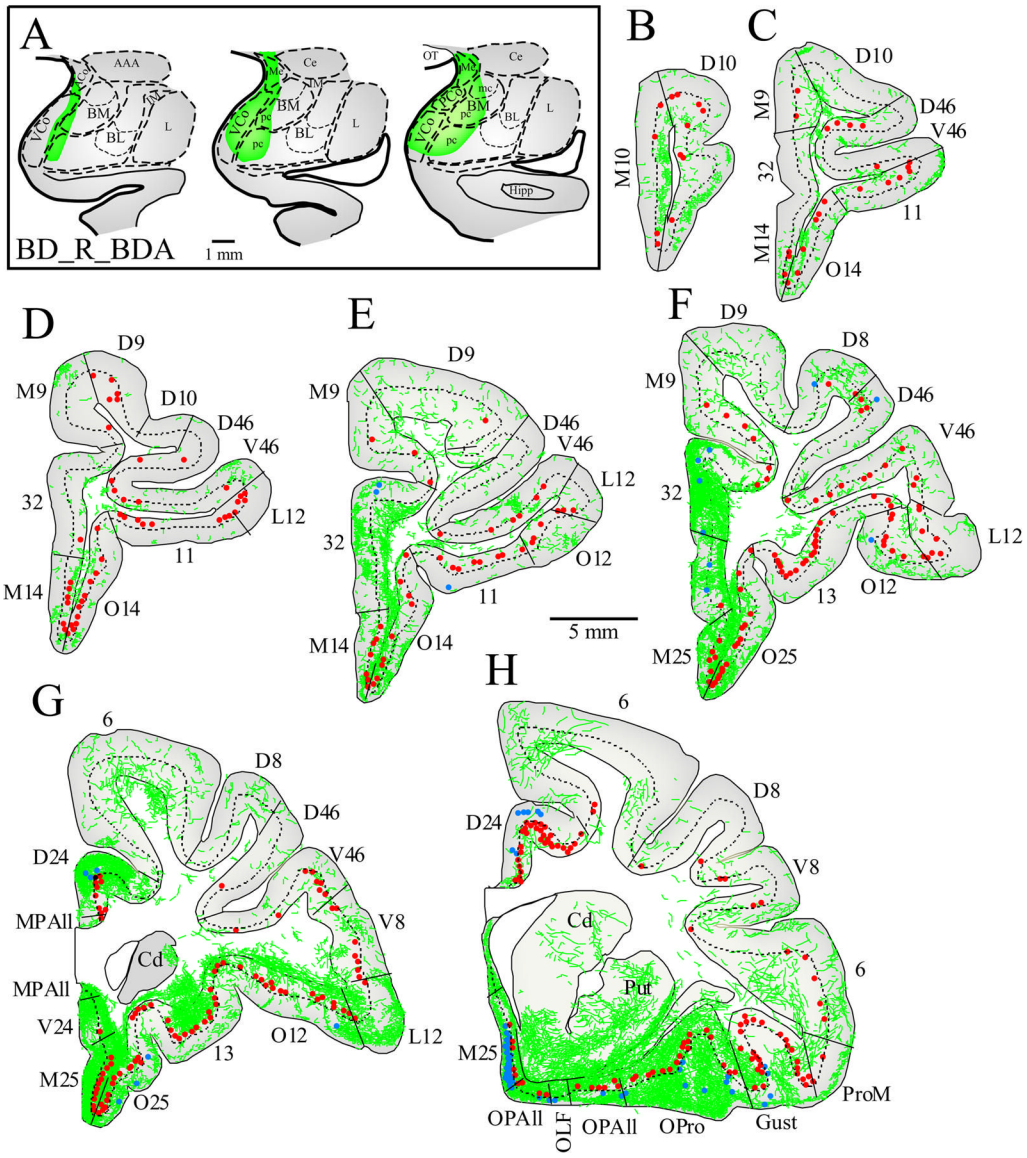

Figure 3. Pattern of input and output connections linking the right prefrontal cortex with the right amygdala

A Rostral (left) to caudal (right) coronal sections through the amygdala showing BDA injection sites in the medial part of BL, BM (also known as accessory basal) and in the cortical nuclei (green area; case BDr). ***B-H***, Coronal sections through rostral (B) to caudal (H) levels of the prefrontal cortex showing the distribution of labeled neurons directed to the amygdala in the superficial (blue dots) and deep (red dots) layers, and labeled axonal terminals (green fibers) from the amygdala. The dotted line through the cortex marks the top of layer 5. Medial is to the left.

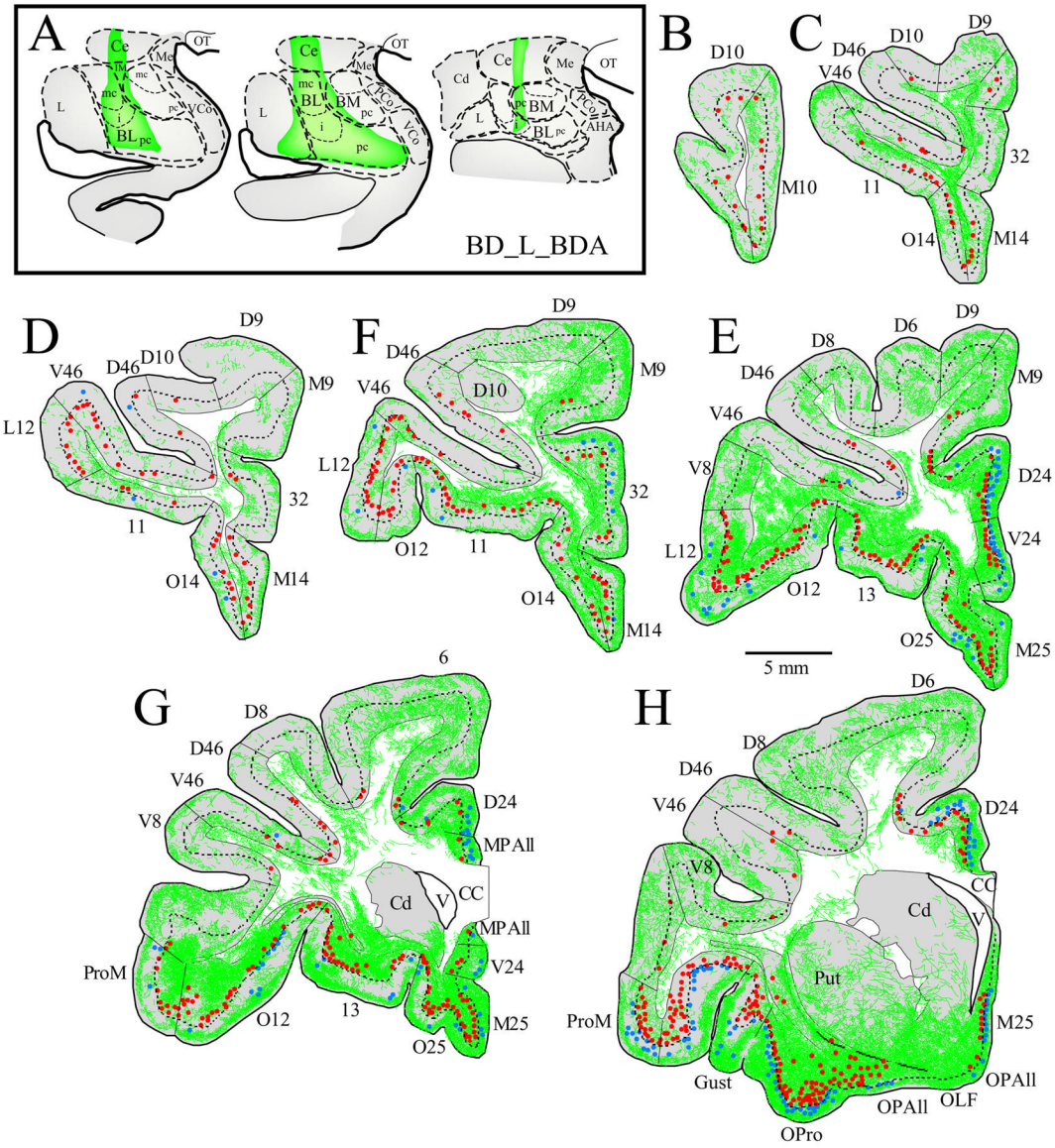

Figure 4. Pattern of input and output connections linking the left prefrontal cortex with the left amygdala

A, Coronal sections through rostral (left) to caudal (right) levels of the amygdala showing the BDA injection, in the BL, Ce and cortical nuclei and the intercalated masses (green area). ***B-H***, Coronal sections through rostral (B) to caudal (H) levels of the prefrontal cortex showing the distribution of labeled neurons directed to the amygdala in the superficial (blue dots) and deep (red dots) layers, and labeled axonal terminals (green fibers) from the amygdala (case BDl). The dotted line through the cortex marks the top of layer 5. Medial is to the right.

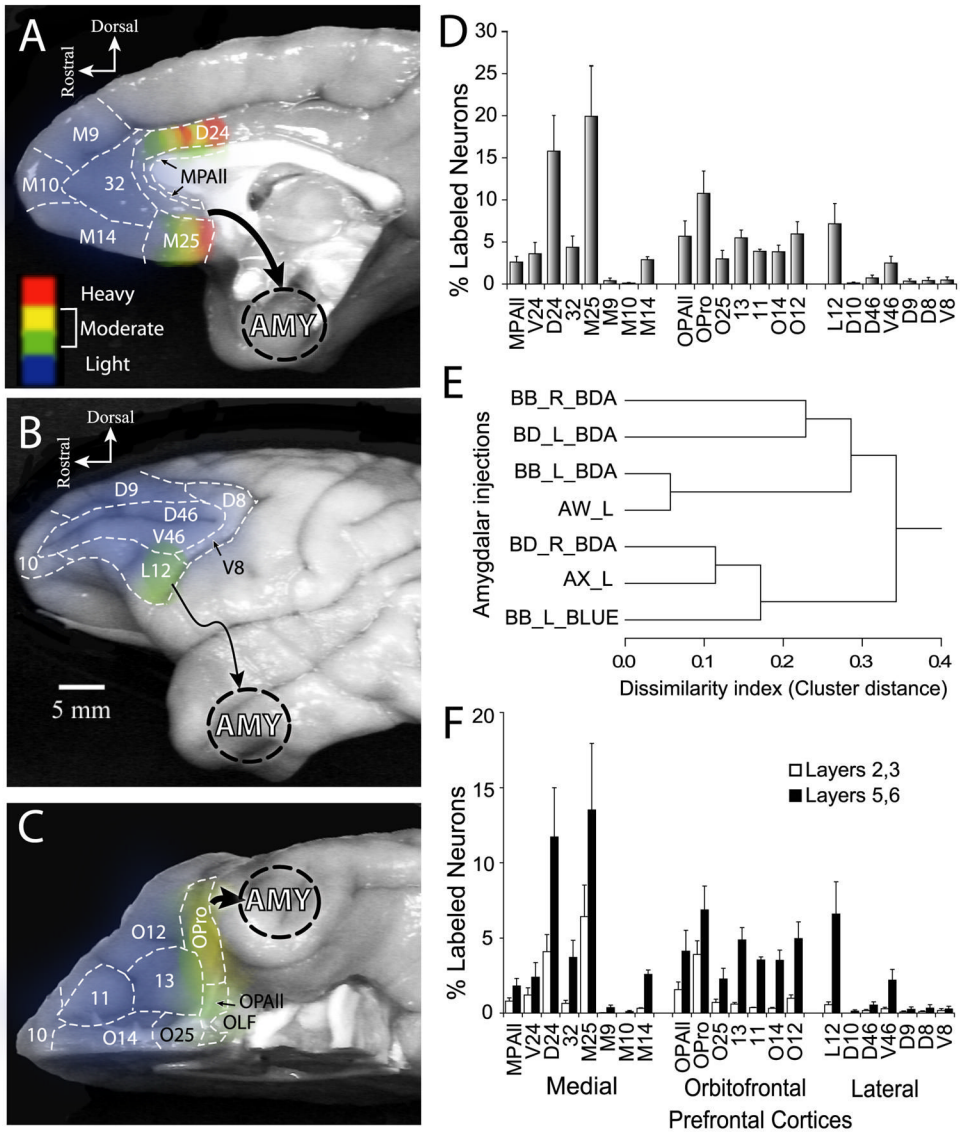

Figure 5. Distribution and density of output projections from the prefrontal cortex to the amygdala

A-C, Density map of projection neurons in prefrontal cortices directed to the amygdala. Grouped densities from all cases were converted to pseudo color and mapped onto photographs of the medial (A), lateral (B), and orbitofrontal (C) surfaces of the prefrontal cortex. Blue-green-yellow to red scale indicates increase in density of projection neurons based on the percentage of the total number of labeled neurons found in prefrontal cortices and averaged across cases. ***D***, Normalized areal distribution of projection neurons in the prefrontal cortices (x-axis) expressed as percentage of total labeled neurons (y-axis) averaged across 7 injection sites. Sum of all bars, 100%. ***E***, Cluster tree diagram of amygdala injections based on the retrograde labeling of projection origins in prefrontal cortices. Projection patterns were evaluated as normalized densities (relative to the total number of neurons labeled by an injection), and similarities between the injections were assessed by Pearson's correlation of all areas' patterns. The diagram indicates two main clusters of similar injections, in regions of the medial nuclei and the BL nucleus, respectively. ***F,*** Superficial and deep laminar contribution of output projections from each area of the prefrontal cortex. Data are percentages of projection

neurons as in D, separated into layers 2,3 (silhouette bars) and layers 5,6 (black bars). Sum of all bars, 100%.

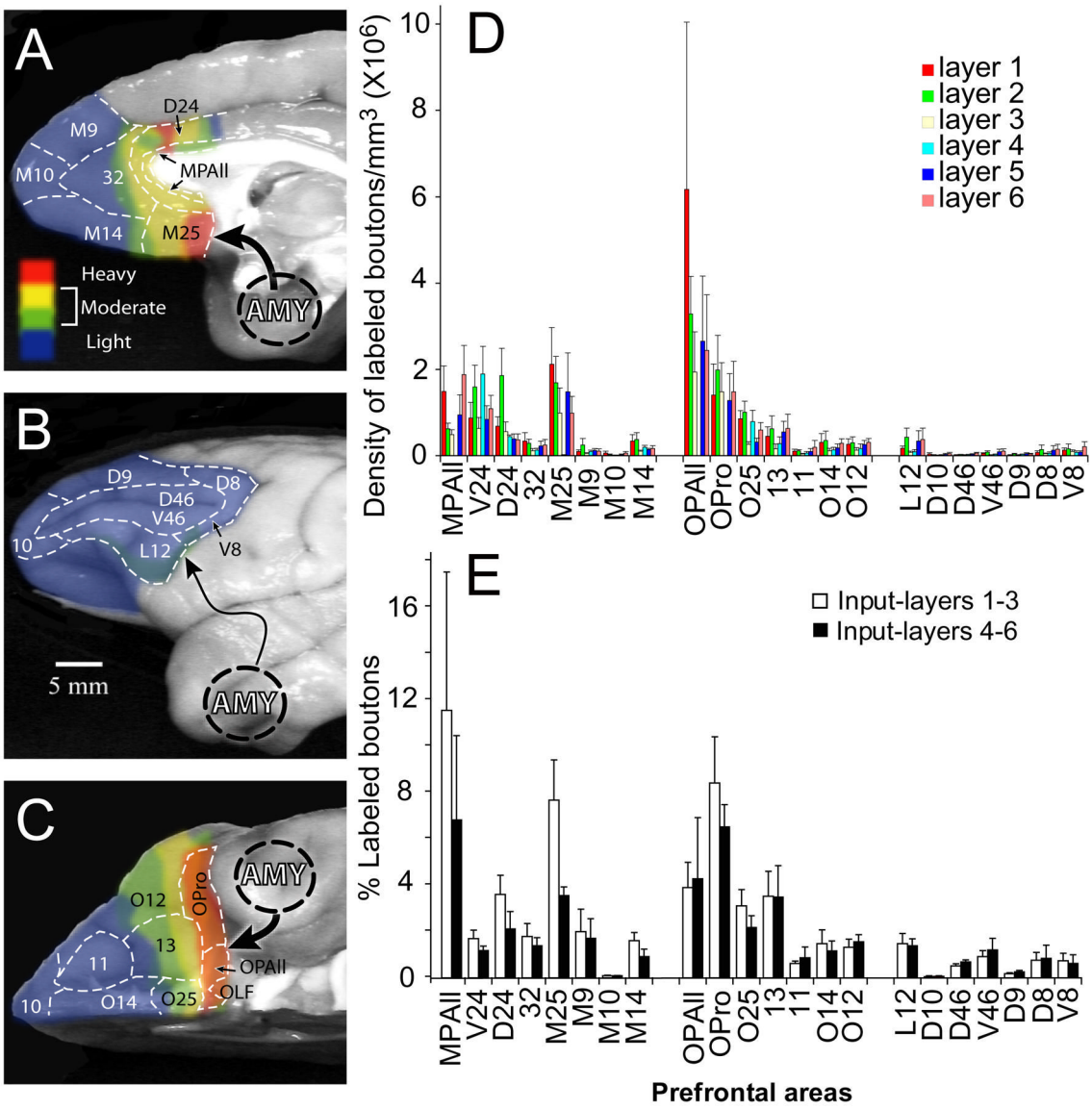

Figure 6. Distribution and density of axonal terminals from the amygdala in prefrontal cortices

A-C, Density of boutons from axons originating in the amygdala and terminating in prefrontal cortices. Densities were converted to pseudo color and mapped onto photographs of the medial (A), lateral (B), and orbitofrontal (C) surfaces of the frontal lobe. Blue-green-yellow to red scale indicates increase in density of axonal boutons based on the percentage of the total number of estimated boutons found in the prefrontal cortices and averaged across cases. ***D,*** Average density of axonal terminations from the amygdala in individual layers of prefrontal cortices in four cases. ***E***, Normalized density of terminations of axonal boutons from the amygdala in the superficial (1−3, silhouette bars) and deep (4−6, black bars) layers of prefrontal cortices in four cases. Density in layers is expressed as percent of total density of boutons in each area. Sum of all bars in D and E, respectively, 100%.

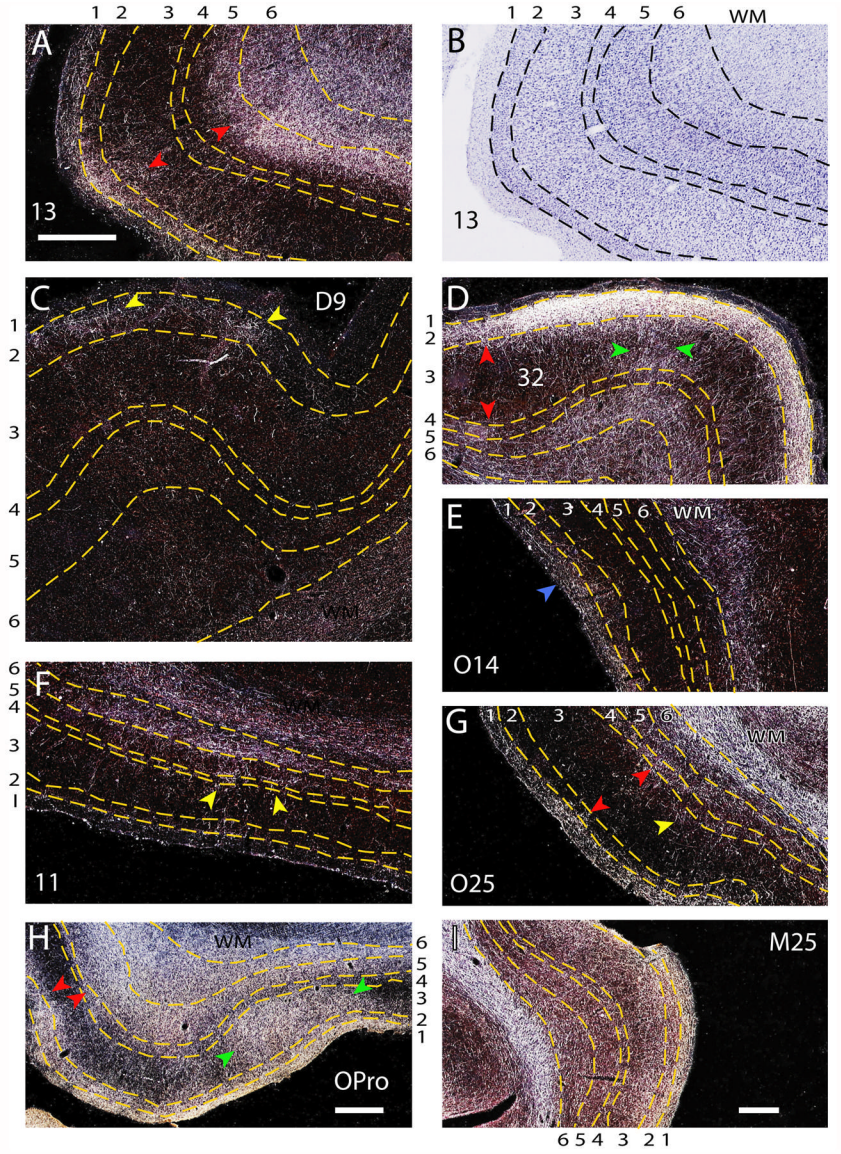

Figure 7. Patterns of axonal terminations from the amygdala in prefrontal cortices

A, Darkfield photomicrograph showing bilaminar distribution of axonal terminals (red arrowheads) in orbitofrontal area 13. Numbers outside the panels indicate the layers (demarcated with dotted lines). ***B***, Brightfield photomicrograph of tissue in A, counterstained with Nissl (blue) to delineate architectonic and laminar borders. ***C,*** Patchy distribution of axonal terminals in layer 2 of dorsolateral area 9 (arrowheads). ***D,*** Bilaminar pattern of innervation in the superficial and deep layers (red arrowheads), and an adjacent column of axonal terminals (green arrowheads) in medial area 32. ***E*** Distribution of axonal terminals in layer 1 of area O14 (blue arrowhead). ***F*** Patchy distribution of axonal terminals in the middle and deep layers of area 11 (arrowheads). ***G***, Bilaminar distribution of axonal terminals in area O25, seen mostly in layers 1, and 4−6 (red arrowheads), with small patch of innervation in the middle layers (yellow arrowhead). ***H***, Column of axonal terminals in caudal orbitofrontal area OPro (green arrowheads) and an adjacent bilaminar pattern of innervation (red arrowheads). ***I***, Distribution of axonal terminals in all layers of area M25. Scale bars = 0.5 mm (A-I). Bar in A applies to B-G.

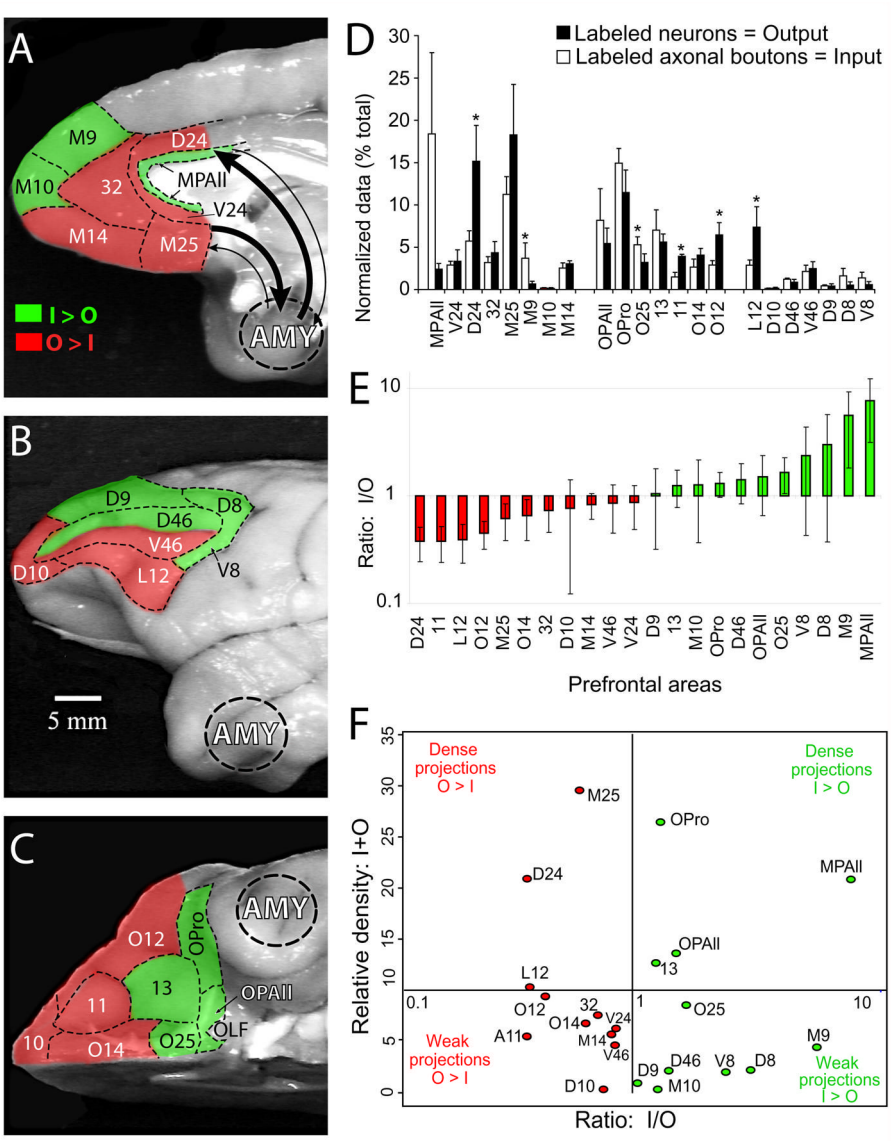

Figure 8. Relative proportion of input and output connections in prefrontal cortices linking them with the amygdala

Prefrontal areas with input from the amygdala greater than output to the amygdala (I>O, green) and O>I (red) are shown on: ***A***, medial; ***B,*** lateral; ***C***, orbital surfaces of the prefrontal cortex. Normalized data obtained from total numbers of labeled projection neurons and axonal terminals in the prefrontal cortex were used for comparison of the relative participation of each prefrontal area as a "sender" (red) or "recipient" (green) of connections with the amygdala. ***D***, Average proportions of axonal boutons originating in the amygdala (input, silhouette bars) and projection neurons directed to the amygdala (output, black bars) in all cases. Sum of the same type bars in D, 100%. Significant differences between the strengths of input and output were assessed by t-tests and are indicated by asterisks. ***E,*** Density ratio for projections from the amygdala to prefrontal cortices relative to reciprocal projections from prefrontal areas to the amygdala (I/O). Green shows areas receiving more input than sending output, and red shows the reverse relationship. Error bars represent S.E.M. from all injection sites. Note that the y-axis uses log scale. ***F***, Input – output ratio (I/O) and relative density (I+O) of prefrontal-amygdala connections. The ratio of relative density of input and output projections, on the x-

axis, is derived as in (E). The x-axis uses a log scale. The density of connections between amygdala and prefrontal cortex, displayed on the y-axis, was evaluated as the sum of the relative input and output densities.

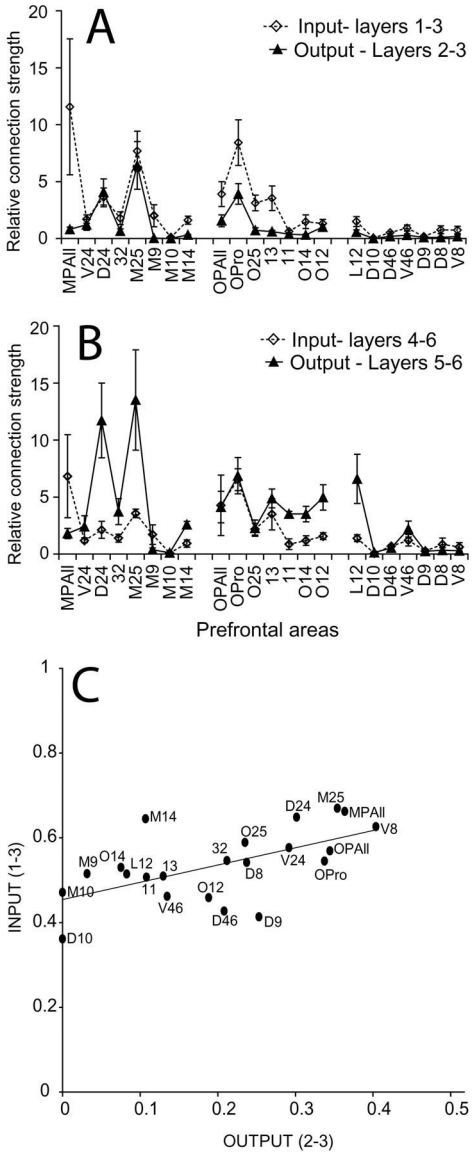

Figure 9. Relationship of laminar-specific input to output connections linking prefrontal cortices with the amygdala

A, Average proportion of axonal boutons from the amygdala terminating in layers 1−3 (diamonds, dotted line) of prefrontal cortices, and output projection neurons from prefrontal cortical layers 2−3 (triangles, solid line) directed to the amygdala, shown for each prefrontal area (x axis). ***B***, Average proportion of axonal boutons from the amygdala terminating in layers 4−6 (diamonds, dotted line) of prefrontal cortices, and output projection neurons from prefrontal cortical layers 5−6 (triangles, solid line) directed to the amygdala. A and B show data from Figure 8D, parceled by laminar compartments. ***C***, Correlation of input from the amygdala to the superficial layers (1-upper 3) of prefrontal cortices (input, y axis) to output projection neurons from prefrontal cortical layers 2−3 (output, x axis) directed to the amygdala. Data are represented as normalized laminar patterns, relative to the sum of neurons or boutons labeled across all layers of an area. The plotted line indicates best linear fit (r=0.60, P=0.003).

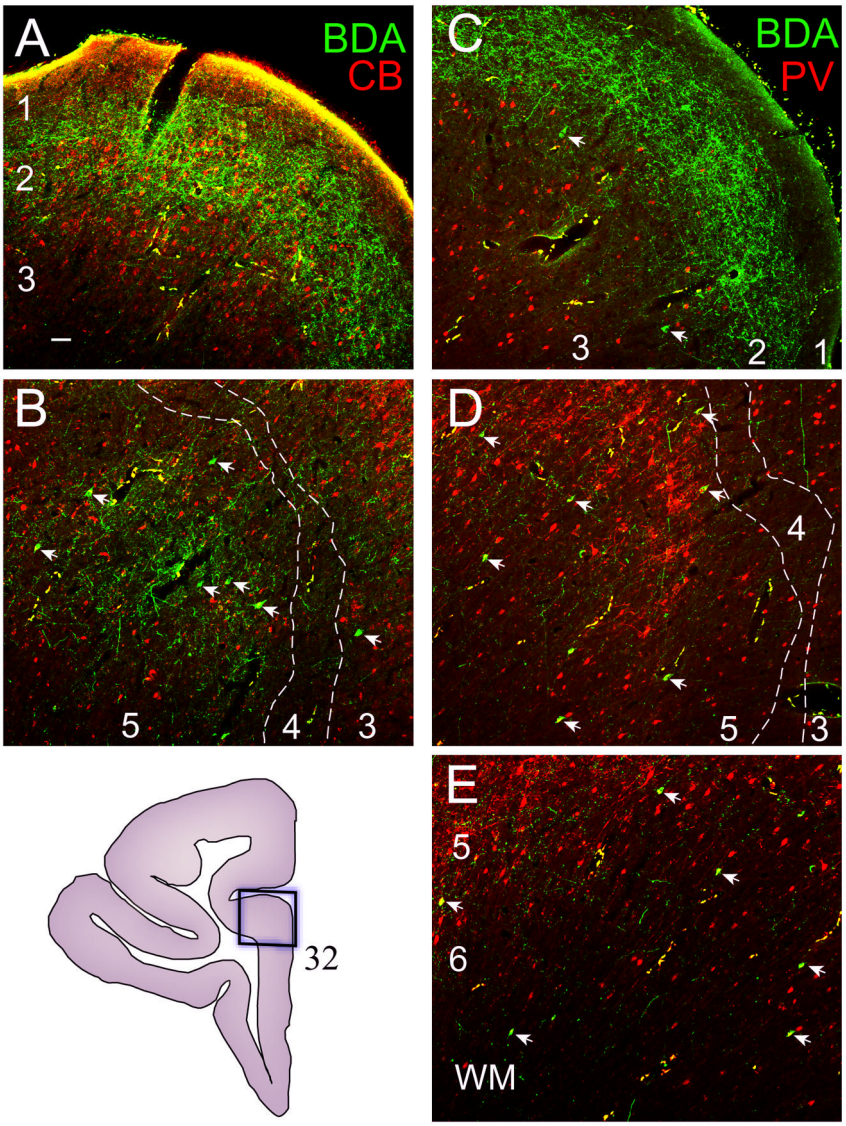

Figure 10. Prefrontal connections with the amygdala overlap with the neurochemical classes of calbindin (CB) and parvalbumin (PV) positive inhibitory neurons in prefrontal cortices

A, Axonal terminals from the amygdala (green fibers) predominantly overlapped with CB positive interneurons (red neurons) in layers 2 and superficial part of layer 3. ***B***, There was little overlap of axons from the amygdala and CB positive interneurons in the middle layers (deep part of layer 3, layer 4, or upper part of layer 5). ***C-E***, PV-positive interneurons (red) were found mostly in the middle layers (deep part of layer 3, layer 4, and superficial part of 5). Projection neurons directed to the amygdala (green neurons, arrows) were surrounded by both CB (B) and PV (D) positive interneurons in the middle layers. Projection neurons (green) in the deep layers were mostly surrounded by PV (red) positive interneurons (E). Inset (bottom left) shows the site (box) where samples from A-E were captured through the depth of the cortex (area 32).

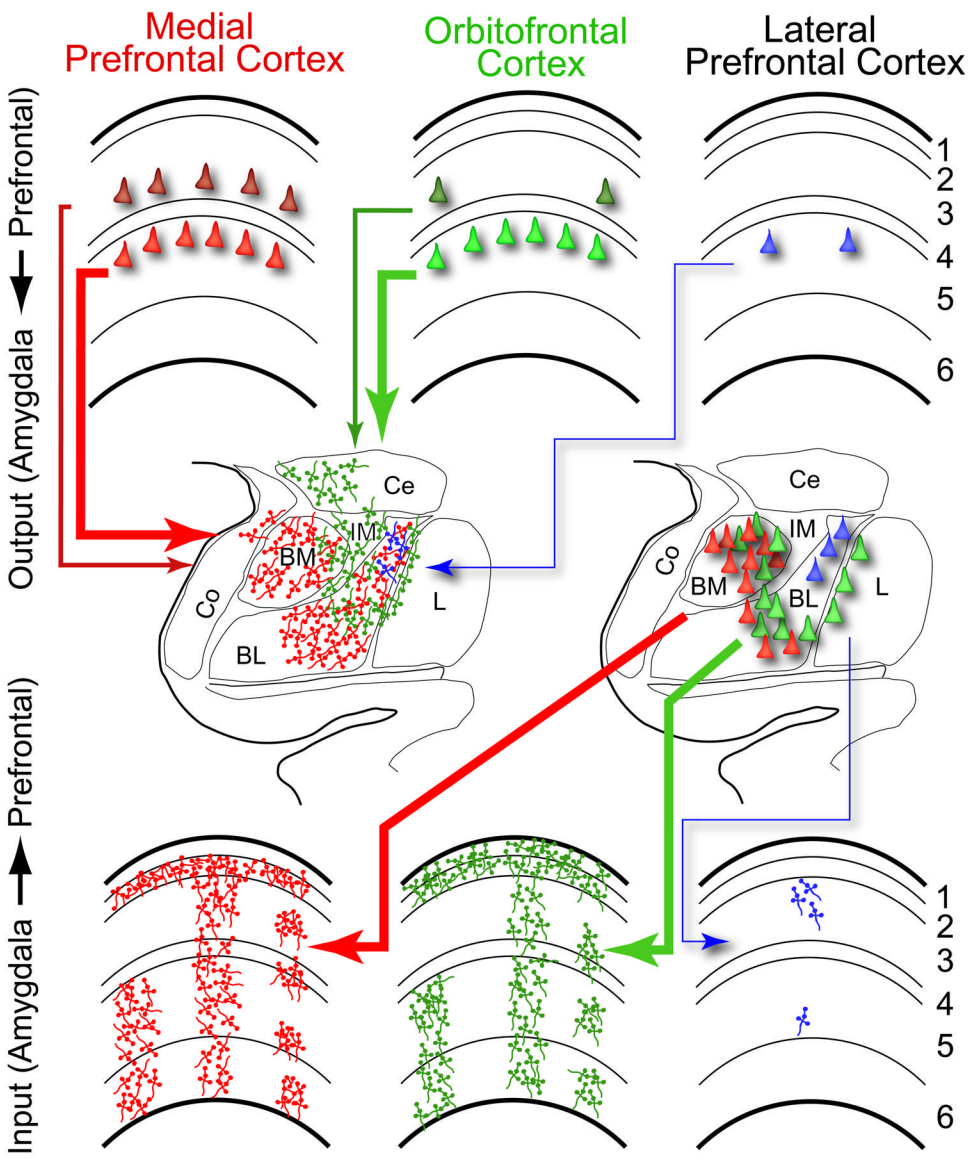

Figure 11. Summary of the output and input patterns of connections of prefrontal cortices with the amygdala

Output projection neurons in prefrontal cortices (top) directed to the amygdala (center) originated mostly in layer 5. Medial and orbitofrontal cortices also issued a significant number of projections from layers 2−3, in contrast with lateral prefrontal cortices. Axons from the amygdala terminated densely in medial and orbitofrontal cortices (bottom), in two bands, including a dense band in layer 1 and another band in the deep layers, columns throughout the layers of the cortex, and patches centered in several cortical layers, including layer 4. In contrast, amygdalar terminations in lateral prefrontal cortices were comparatively sparse and patchy in the superficial or deep layers. The middle frames summarize the pattern of terminations from prefrontal cortices to the amygdala (left center) and the origin of projection neurons from the amygdala to prefrontal cortices (right center) obtained in a previous study (Ghashghaei and Barbas, 2002). The thickness of the arrows signifies strength of connection, and the number of neurons depicts their relative density.

Table 1

Cases, injection sites, the type of dyes used, the hemisphere of injection in the amygdala, and the amount injected

	Case	Amygdalar nuclei included in the injection sites	Dye	Hemisphere	Amount Injected
Rostral half of Amygdala	BBr[¶#]	BMpc, AAA[*], BLpc[*], BLi, IM, ACo	BDA	Right	10 μl
	BBl[¶#]	AAA, BMmc[*], BMpc[*], BLi, BLpc	BDA	Left	10 μl
	BBb[¶]	ACo, nLOT, BMpc, BLpc[*]	Fast Blue	Left	3 μl
	AW[¶]	L[*], BLpc[*]	Fluororuby	Left	1.5 μl
Caudal half of Amygdala	AX[¶]	BMpc[*], BMmc[*]	Fluororuby	Left	2.5 μl
	BDr[¶#]	Me[*], BMmc, BMpc, BLpc, PCo[*], VCo[*]	BDA	Right	10 μl
	BDl[¶#]	Ce, BLmc[*], BLi[*], BLpc[*]	BDA	Left	10 μl

[#] Anterograde analysis

[¶] Retrograde analysis

[*] Nuclei that included most of the injection site in each case